

10  
5-12-94 JSD

LBL-35374  
UC 109

Center for Advanced Materials

# CAM

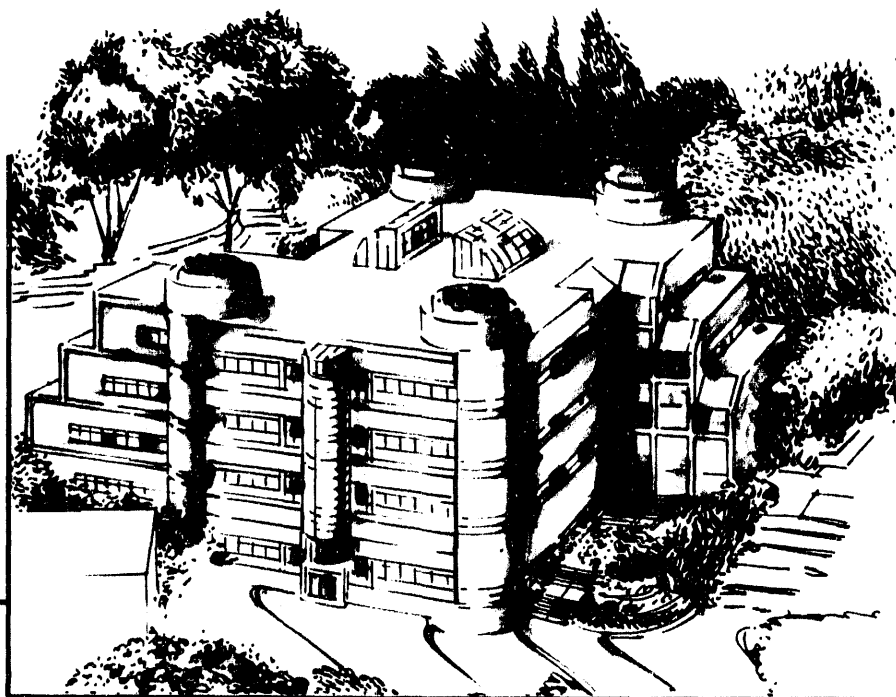
**Fundamental and Exploratory Studies of Catalytic  
Steam Gasification of Carbonaceous Materials**

**Final Report**

**Fiscal years 1985-1994**

**H. Heinemann and G.A. Somorjai**

**March 1994**



**Materials and Chemical Sciences Division**  
**Lawrence Berkeley Laboratory • University of California**  
**ONE CYCLOTRON ROAD, BERKELEY, CA 94720 • (415) 486-4755**

Prepared for the U.S. Department of Energy under Contract DE-AC03-76SF00098

**DISTRIBUTION OF THIS DOCUMENT IS UNLIMITED**

LBL-35374  
UC 109

**FUNDAMENTAL AND EXPLORATORY STUDIES  
OF CATALYTIC STEAM GASIFICATION  
OF CARBONACEOUS MATERIALS**

Final report covering fiscal years 1985-1994

Principal Investigators: Heinz Heinemann  
Gabor A. Somorjai

Center for Advanced Materials  
Materials Sciences Division  
Lawrence Berkeley Laboratory  
University of California  
Berkeley, CA 94720

-----  
This work was supported by the Assistant Secretary for Fossil Energy,  
Office of Technical Coordination, U.S. Department of Energy under  
Contract DE-AC03-76SF00098, through the Morgantown Energy  
Technology Center, Morgantown, West Virginia 26505.

**MASTER**

DISTRIBUTION OF THIS DOCUMENT IS UNLIMITED *ee*

## TABLE OF CONTENTS

	Page
<b>I. OBJECTIVE</b>	1
<b>II. EXECUTIVE SUMMARY</b>	
A) Gasification of Graphite	1
B) Gasification of Coals, Chars and Petroleum Cokes	2
<b>III. INTRODUCTION</b>	4
<b>IV. BACKGROUND</b>	4
<b>V. EXPERIMENTAL</b>	
A) Equipment	5
B) Catalysts	7
C) Operating Conditions	7
<b>VI. RESULTS</b>	
A) Catalytic Steam Gasification of Graphite	
1) Alkali or Earth Alkali Catalysts	8
2) Binary Catalysts	13
3) Mechanism of the Graphite-Catalyst-Steam Interaction	22
B) Steam Gasification of Chars	
1) Potassium-Nickel Oxide Catalysts	31
2) Potassium-Calcium Oxide Catalysts	37
3) Ternary Catalysts	44
4) Operation at Elevated Pressure	45
5) Chars Prepared in the Presence of Alkali	47
6) Use of Alkali by Steam Entrainment	50
C) Steam Gasification of Coals	
1) Kinetics	53
2) Catalyst Modifications	58
D) Steam Gasification of Petroleum Cokes	62
<b>VII. CONCLUSIONS</b>	66
<b>VIII. REFERENCES</b>	67
<b>IX. APPENDIX</b>	
Publications of Work Performed Under This Contract	68
<b>X. ACKNOWLEDGEMENTS</b>	70

## **I. OBJECTIVE**

The major purpose of this project was to find catalysts which will permit steam gasification of carbonaceous material at reasonable rates and at lower temperatures than currently practiced. Rapid catalyst deactivation must be avoided. An understanding of the catalytic mechanism is necessary to provide leads towards this aim.

## **II. EXECUTIVE SUMMARY**

### **A) Gasification of Graphite**

It must be assumed that results of experiments with graphite can be extrapolated to coal and chars. The latter substances are not suitable for investigation by high-vacuum techniques.

- Experiments with steam gasification of graphite in the presence of alkali compounds confirm that at relatively low temperatures (below 600 °C), a stoichiometric reaction occurs between carbon, alkali and water, forming a phenoxide and hydrogen. The reaction stops when all alkali has been used. At higher temperatures the phenoxide decomposes giving CO<sub>x</sub> and alkali hydroxide.
- The decomposition of the phenoxide can be accomplished at low temperatures using a transition metal oxide as a catalyst. Mixtures of an alkali oxide and a transition metal oxide can serve as catalysts for continuous steam gasification of graphite (and chars and coals) at temperatures below 600 °C. Preferred combinations are mixtures of potassium and nickel oxides. Sodium and iron oxide may be used.
- Work in the controlled atmosphere chamber of an electron microscope has shown that alkali compounds alone attack carbon in the presence of water in a solid particle-graphite edge contact, leading to channeling. Alkali-transition metal oxide mixtures form low melting eutectica, resulting in a liquid film which attacks the graphite by edge recession. The rate of gasification is much higher for the binary mixture.
- Gasification of carbonaceous materials with steam in the presence of a binary oxide catalyst requires that the catalyst can dissociate water at the gasification temperature. Hydrogen is released and oxygen forms a surface oxide with the carbon,

such as a quinone or lactone, which then decomposes, thermally giving  $\text{CO}_x$ .

#### **B) Gasification of Coals, Chars and Petroleum Cokes**

- Steam gasification in the presence of a binary oxide catalyst produces hydrogen and carbon dioxide in a 2:1 molar ratio with only minor amounts of CO and traces of methane. The larger-than-equilibrium  $\text{CO}_2/\text{CO}$  ratio is probably due to a shift reaction.
- Binary oxide catalysts containing a transition metal oxide such as  $\text{K-Ni-O}_x$  are poisoned by sulfur compounds. In the steam gasification of coals, it has been shown that poisoning occurs with organic sulfur but not with pyritic sulfur in the coal.
- It was found that mixtures of an alkali compound with an earth alkali oxide, such as Ca-K-oxide, possess the same characteristics as, for example,  $\text{K-Ni-O}_x$  catalysts for gasification. Equimolar mixtures of potassium and calcium oxide are only slightly less active than  $\text{K-Ni-O}_x$  but are much more poison-resistant.
- Some ternary oxides, such as K-Ca-Co oxide, are more active for steam gasification than the binary oxides.
- The catalysts are preferentially used in a carbon to binary oxide molar ratio of 1:0.04. They can be applied to the coal or char by impregnation or just by physical mixing.
- A series of chars and of coals were gasified with steam in the presence of binary oxide catalysts. In general, coals gasify faster than chars and chars gasify faster than graphite. Complete gasification of the carbon content is obtained. The rate of gasification declines from lignite > subbituminous > bituminous coals.
- While most gasification experiments were carried out at atmospheric pressure, the steam gasification rate was not enhanced by operating at 100 psig.
- Ash components in coals other than sulfur do not appear to greatly affect the catalysis.

- Charring coals or coking petroleum resid in the presence of small amounts of alkali resulted in chars or cokes which were much easier to gasify than the chars or cokes prepared in the absence of alkali. Gasification with catalysts further enhanced the gasification rate.
- A number of petroleum cokes were catalytically gasified with steam. They behaved much like coals. There appeared to be no major effect of varying metal content of the cokes.
- Introduction of alkali during gasification with the steam (by entrainment) gave similar results to those obtained by charring or coking in the presence of alkali.
- The amounts of catalyst used can be reduced and it may be possible to use the catalyst on a throw-away basis and not recover it from the ash.

### III. INTRODUCTION

This project, Fundamentals of Catalytic Gasification, has been carried out at the Lawrence Berkeley Laboratory during the fiscal years 1985-1994. It has been supported by the Assistant Secretary for Fossil Energy, Office of Technical Coordination, U.S. Department of Energy under Contract DE-AC03-76SF00098, through the Morgantown Energy Technology Center, Morgantown, West Virginia 26505. Results which are summarized in this report have previously been reported in greater detail in quarterly and annual reports and in a number of publications which are listed in the Appendix. This report is a modified and enlarged version of a summary report (LBL-30015) issued in 1990 and includes work performed in 1990-1993.

### IV. BACKGROUND

The production of synthesis gas by reaction of various carbonaceous materials with steam has been frequently investigated and is a commercial process. Gasification in the presence of alkali metal compounds has been reviewed by WEN [1]. The mechanism of the catalytic gasification of coal chars has been reviewed by WOOD and SANCIER in 1984 [2]. The production of low molecular weight gaseous hydrocarbons directly from carbon or from carbonaceous materials provides an intriguing alternative to syngas production with subsequent methanation or liquefaction. The reaction of carbon with water to reproduce methane and carbon dioxide,  $2C + 2H_2O \rightarrow CH_4 + CO_2$ , is virtually thermoneutral ( $\Delta G_{298K} = 2.89$  Kcal/mol) and thermodynamically feasible at low temperatures. By contrast, studies of coal gasification with water have always been carried out at high temperature regimes in order to have efficient production of carbon monoxide and hydrogen, a very endothermic reaction. More recent studies by Exxon researchers [3] reported the production of substantial amounts of methane along with CO and hydrogen during coal gasification using potassium carbonate as a catalyst. These studies employed relatively high temperatures (630-830 °C).

## V. EXPERIMENTAL

### A) Equipment

The work carried out in this project involved primarily three types of equipment:

- 1) A flow reactor as shown in FIG. 1. This type of reactor system with either a horizontal or a vertical reactor and furnace was used for all kinetic studies. A modified reactor, shown in FIG. 2, was used for studies at elevated pressure.
- 2) A high pressure-low pressure ultra-high vacuum cell [4], operating at a base pressure greater than  $10^{-9}$  torr (FIG. 3). It is equipped to determine surface composition analysis by Auger electron spectroscopy and by XPS. The system is also equipped with a high pressure cell which isolates the sample and permits the performance of chemical reaction studies at high pressure without removing the sample from the UHV chamber. The product distribution is monitored by gas chromatography with a thermal conductivity detector.
- 3) A controlled atmosphere electron microscope (CAEM). All work in this equipment was with graphite to prevent fogging of the chamber which would occur with coals or chars.

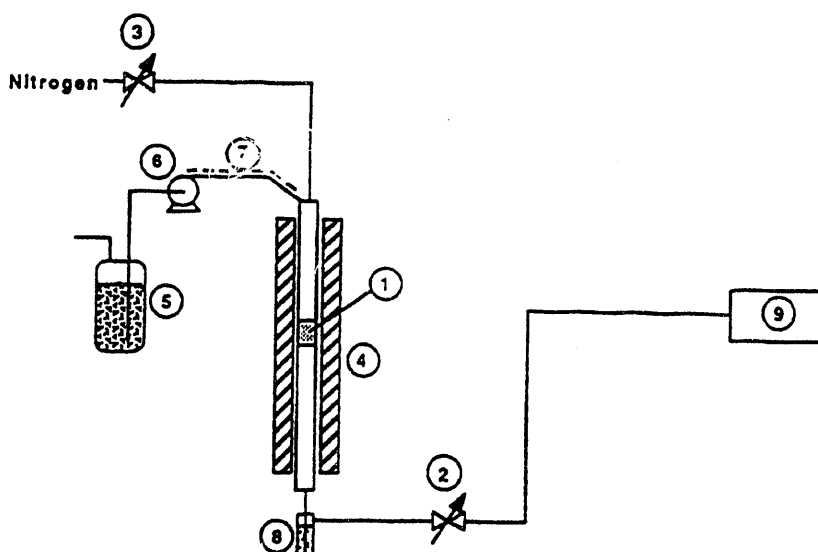


FIG. 1. Reactor setup: (1) reactor; (2) back pressure regulator; (3) mass flow controller; (4) furnace; (5) reservoir; (6) pump; (7) heating tape; (8) condenser; and (9) gas chromatograph.



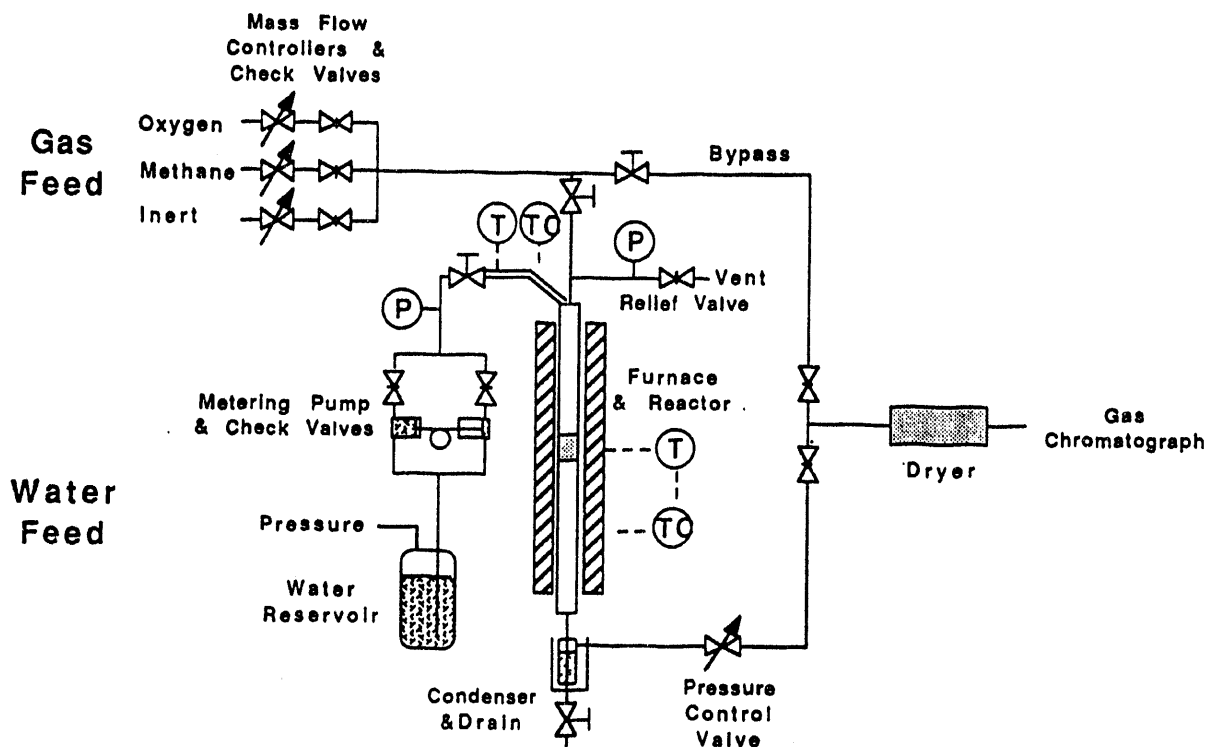


FIG. 2.

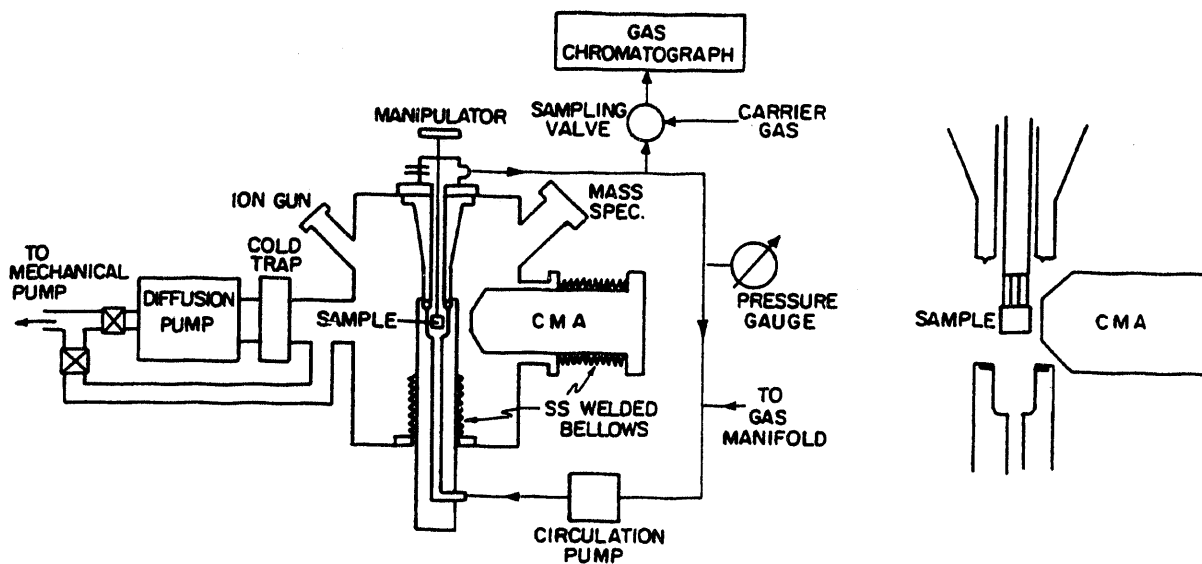


FIG. 3. High pressure-low pressure ultra-high vacuum cell.

Transparent flakes of graphite were prepared by attaching the graphite to a glass slide using low-melting-point wax and repeatedly cleaving the graphite along its basal plane with adhesive tape until only a small section was left stuck to the glass slide. The section was released using acetone, picked up on a gold 500-mesh grid and allowed to dry in air. The graphite was then impregnated with K and/or Ca nitrate and the flow reactor system described was used to decompose the salts.

Unless otherwise described, the experiments were performed in a KRATOS EM-1500 transmission electron microscope at the National Center for Electron Microscopy at the Lawrence Berkeley Laboratory.

A Gatan single-tilt heating stage was used in a Gatan environmental cell. Argon was bubbled through water and the water vapor/argon mixture was fed directly into the cell at a pressure of 3 torr. The microscope was operated at its maximum accelerating voltage, 1.5 MeV, and dynamic images were displayed and recorded via a video camera.

A detailed description of the CAEM technique can be found elsewhere [5].

## **B) Catalysts**

Catalysts used in this work were primarily mixtures of alkali and transition metal oxides, and of alkali and earth alkali oxides. Some ternary catalyst mixtures were also tested. For comparison purposes, alkali oxides alone were used. The preferred alkali was potassium, although sodium was found to possess equivalent activity. The preferred transition metal was nickel and the preferred earth alkali was calcium.

The catalysts were prepared by mixing aqueous solutions of the nitrates and impregnating the carbonaceous substrate with the solution to deposit 1-3 mol % of the mixed oxide. The impregnated carbon was dried and the nitrate decomposed by heating. It was found that hydroxides, carbonates and oxalates could be employed with equal catalyst efficiency, but that for carbonates, a calcination temperature above 900 °C was required to convert the carbonate to oxide. The preferred catalyst-to-carbon ratio was 0.04.

The mixed catalysts had eutectic melting points and at the usual operating temperature (525-630 °C), formed a liquid film on the substrate. It was even possible to mix the dry salts, add them to the carbon and heat to reaction temperature.

## **C) Operating Conditions**

All of the work in the flow reactor was at atmospheric pressure, except where indicated differently. The temperature in the impregnated carbon sample was controlled to  $\pm 5$  °C. The range of gasification temperatures was 550-700 °C. Steam was introduced at close to reaction temperature by vaporizing and preheating water charged from a syringe pump at controlled rates. The standard rate of water charged is 8cc/g catalyst/hr.

## VI RESULTS

### A) Catalytic Steam Gasification of Graphite

#### 1) Alkali or Earth Alkali Catalysts.

In this project the gasification of graphite has been studied in the presence of alkali hydroxide and, in some cases, of earth alkali hydroxide at temperatures in the range 230-525 °C and atmospheric pressure. We have used graphite as a carbon source because of its lack of hydrocarbonaceous material and in order to be sure that all hydrogen produced as hydrogen or in hydrocarbons was derived from hydrogen in water.

Early work in the high pressure-low pressure cell indicated that methane could be produced at temperatures as low as 200 °C in the presence of potassium hydroxide [6] as indicated in FIG. 4. FIG. 5 shows the methane production with various alkali hydroxides. While the rate of methane production is low, it becomes appreciable if one assumes that not all the geometric surface area of graphite is available for attack and that the attack probably takes place on the edges of the graphite.

We have carried out gasification studies in the environmental cell of a transmission electron microscope similar to the studies that were previously carried out by BAKER [5], who gasified graphite crystals in the presence of nickel and hydrogen and showed that gasification occurred by "basal plane

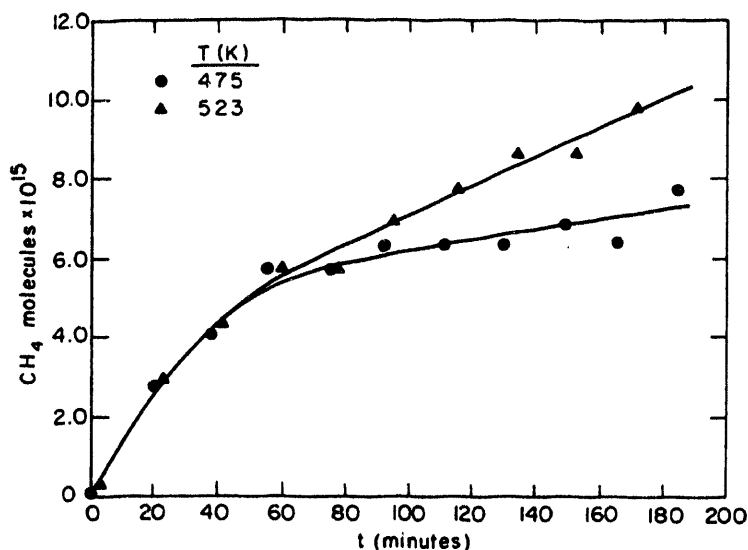


FIG. 4. CH<sub>4</sub> production as a function of temperature in the presence of KOH.

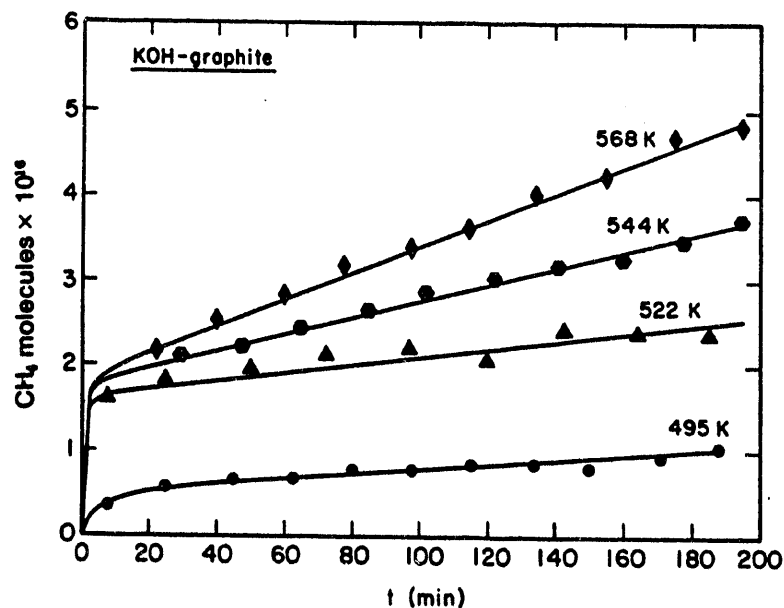


FIG. 5. CH<sub>4</sub> production with various alkali hydroxides.

penetration in imperfect regions or by altering the rate of reaction at edges or steps". In our studies, thin specimens of highly-oriented pyrolytic graphite were obtained by cleavage of graphite crystals. Potassium hydroxide was introduced onto the surface of the graphite by dipping the specimen supported on copper or nickel grids into a 0.38M solution of potassium hydroxide and then dried. Transmission electron microscopy was carried out in a Hitachi 650 keV microscope [7]. Argon at about 1 atm pressure was bubbled through water at room temperature, giving an argon/water ratio of about 40:1 and then introduced into the environmental cell to give a pressure of 50 Torr. At 500 °C the potassium hydroxide was dispersed as particles of 0.1 to 0.5 microns in diameter on the surface of the graphite. FIGS. 6 and 7 show micrographs recorded 10 minutes apart taken from a sequence showing the channel growth at 770K. Channels are evident in two adjacent graphite crystals emanating from the edges of the crystal, each channel with a particle at its head. As the reaction continues, the particles move and the length of the channels increase. The channels remain roughly parallel-sided, indicating that there is little effect of uncatalyzed reaction at the channel edges or of wetting of the channel sides by catalytic material. Intercalation of potassium into the graphite does not appear to play a role in the gasification. Samples of potassium intercalated graphite (C<sub>24</sub>K) were subjected to reaction with water at 300 °C and exhibited an appreciably lower methane production than graphite impregnated with potassium hydroxide [8]. Both AES



FIG. 6. Micrograph of KOH catalyzed reaction.



FIG. 7. Micrograph of KOH catalyzed reaction ten minutes later.

and XPS studies of potassium intercalated graphite also indicated that potassium diffuses to the surface under the influence of the electron beam. The intensity of the potassium peak decreased upon heating.

It was also observed, when using calcium hydroxide for the gasification of graphite, that a new photoelectron emission peak corresponding to a  $C_{1s}$  electron binding energy of 290 eV is formed, representing a more reactive form of carbon probably in connection with oxygen. As will be shown later, this probably constitutes a phenoxide species also observed by MIMS and PABST [3].

In experiments with the flow reactor, shown in FIG. 1, it was found that two regimens of gas production prevailed, as illustrated in FIG. 8. In the first, hydrogen, methane and higher hydrocarbons were produced with almost no carbon monoxide or carbon dioxide production. In the second regime, hydrogen and CO were produced at a lower rate [9]. The first regime prevails until exactly one-half mole of hydrogen as either hydrogen or in hydrocarbon has been produced per mole of KOH present. This then would indicate that one is dealing with a stoichiometric reaction in which carbon reacts with potassium hydroxide to form a phenoxide and one-half mole of hydrogen which, in turn, may react with carbon to form hydrocarbons. Such a reaction can be described as:  $5C + 4KOH \rightarrow 4COK + CH_4$ . The fact that higher hydrocarbons up to  $C_6$  are also formed is of interest [9]. The presence of the stoichiometric phenoxide compound was confirmed by XPS and was also established by NMR work reported by MIMS and PABST [3].

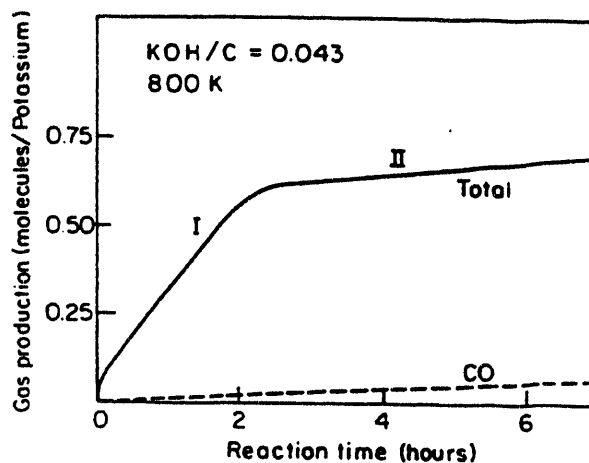


FIG. 8. Gas production in the flow reactor.

When a sample of potassium hydroxide-impregnated graphite which has been reacted to completion of the stoichiometric reaction is heated to about 1025 °C, the phenolate is decomposed with production of carbon monoxide. Following this, gasification at low temperature can again begin in line with regime 1 in FIG. 8.

## 2) Binary Catalysts.

We have found that the overall reaction can be made truly catalytic by adding a co-catalyst to the potassium hydroxide. Suitable materials are metal oxides and particularly nickel and iron oxide, as shown in FIG. 9. It appears that in the presence of the metal oxide, the phenolate is decomposed as quickly as it is formed and gasification occurs at 525 °C at a steady rate, which has been followed up to 25% conversion of the graphite. This is illustrated in FIG. 10. The reaction proceeding can be simulated by the following equations:

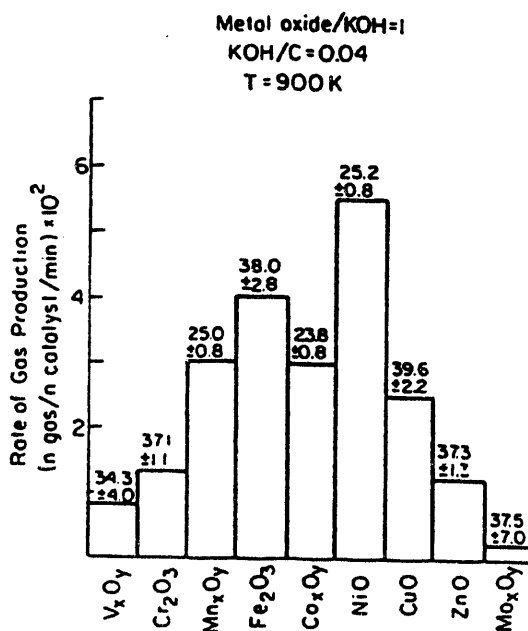
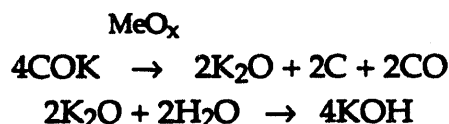


FIG. 9. Gas production and activation energy for various metal oxides. (XBL 851-5706)



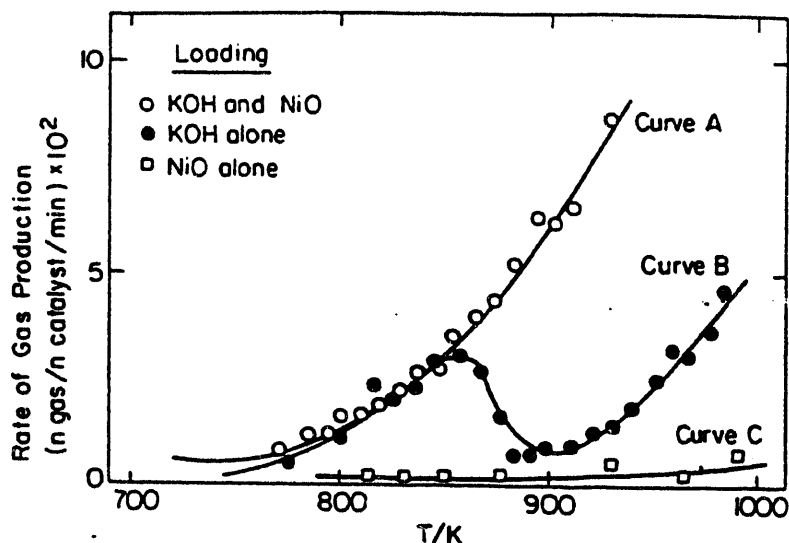


FIG. 10. Temperature-controlled gas production for three catalysts.  
XBL 851-5705

In the gasification with potassium hydroxide plus metal oxide, the products are essentially hydrogen and carbon dioxide in a ratio of 2:1. Only traces of hydrocarbons are found. It was at first suspected that in these reactions methane might be a primary product, which is then steam reformed to CO and hydrogen. Addition of methane to the water feed illustrated, however, that only minor amounts, if any, of steam-reforming take place. Decomposition of methane over the metal oxide may occur to a small extent and this may be the reason why only traces of hydrocarbons are found. The high hydrogen to CO<sub>2</sub> ratio and the absence of carbon monoxide are attributed to a watergas shift reaction proceeding simultaneously with the gasification. We have considered the possibility of a Boudouart reaction with subsequent gasification of the carbon from the disproportionation, but believe it to be less likely than the watergas shift reaction. It is important to note that the production of hydrogen and carbon dioxide in the 2:1 molar ratio allows high hydrogen production directly from the gasification of carbonaceous material without a separate shift reaction, and that the reaction proceeds at temperatures appreciably lower than those previously observed. One must also note that the reaction is carried out at essentially atmospheric pressure and that the kinetics might be improved by operating at higher water partial pressure.

It can be concluded that phenoxide type compounds are formed from the reaction of carbon, water and alkali hydroxide as in-

intermediates in the production of hydrogen and/or of hydrocarbons from carbonaceous material and water in the presence of alkali hydroxides.

Isothermal experiments between 425 °C and 725 °C were performed to determine the product distribution for the gasification of graphite with steam using NiO-KOH as a catalyst. The rate of gas production was similar (within 10%) to those obtained from a temperature-programmed experiment.

In the temperature range studied, the major products were H<sub>2</sub> and CO<sub>2</sub>, with a molar ratio of 2.2 ± 0.5. Although some CO was produced above 625 °C, the amount was one order of magnitude less than the amount of CO<sub>2</sub> produced. These results strongly contrasted with the CO/CO<sub>2</sub> molar ratio calculated at equilibrium conditions. Below 625 °C, CH<sub>4</sub> was produced as a minor constituent and its fraction in the gaseous products decreased with time. At the beginning of the gasification process, the CH<sub>4</sub>/H<sub>2</sub> molar ratio was ≈4 × 10<sup>-2</sup>, but after 4% graphite conversion, it dropped to ≈10<sup>-3</sup>.

In order to prove that the gasification of graphite with steam was indeed catalyzed by KOH-NiO, the gas production was followed under isothermal conditions at 590 °C up to a graphite conversion of 25%. The results are shown in FIG. 11 (curve A). FIG. 11 (curve A) shows that the KOH-NiO catalyst was still active after 24 turnovers, while adsorbed KOH alone on graphite

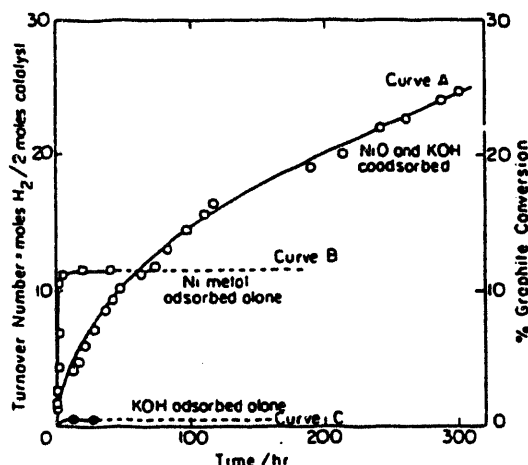


FIG. 11. Turnover number as a function of time for isothermal reactions at 590 °C. The open circles (curve A) correspond to NiO-KOH codeposited on graphite, the open squares (curve B) to Ni metal deposited alone, and the full circles to KOH deposited alone on graphite. In curves A and B, the ratio of Ni:C is 0.01. In curves A and C, the ratio C:K is 0.01. XBL 851-5708

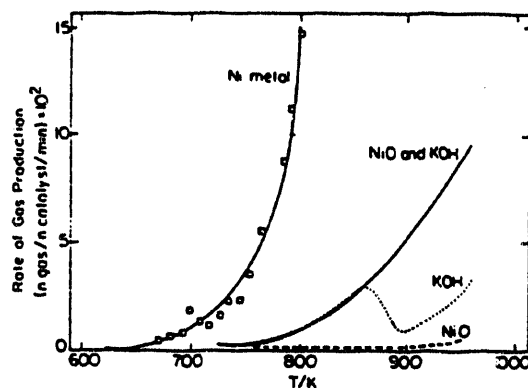


FIG. 12. Plot of the temperature dependence of the gas production rate during a temperature-programmed experiment at a heating rate of  $5\text{K min}^{-1}$ . The open squares correspond to Ni metal deposited on the graphite surface. The ratio of Ni:C is 0.04. The plots for KOH, KOH + NiO, and NiO, shown in detail in FIG. 10, are included for comparison. XBL 851-5709

became inactive after 0.25 turnovers at the same temperature (see FIG. 9, curve C). When NiO only was present as a catalyst on graphite, no gas production was obtained at this temperature after an initial burst.

When KOH and  $\text{Fe}_2\text{O}_3$  were codeposited on graphite, the results obtained were similar to the case when codeposited KOH and NiO were used. Isothermal experiments at  $590^\circ\text{C}$  with  $\text{Fe}_2\text{O}_3$  and KOH coadsorbed on graphite showed that gasification was still occurring at a steady-state rate after 25% graphite conversion and 24 turnovers, although the rate of gas production was smaller than when the NiO-KOH catalyst was used. The major products were  $\text{H}_2$  and  $\text{CO}_2$  with a  $\text{H}_2/\text{CO}_2$  molar ratio of  $2.0 \pm 0.5$ . When  $\text{Fe}_2\text{O}_3$  is adsorbed alone, no gas production is obtained in a temperature-programmed experiment until temperatures above  $825^\circ\text{C}$  are employed.

The catalytic activity for the gasification of graphite with steam of  $\text{K}_2\text{CO}_3$ -NiO coadsorbed on graphite was studied in a temperature-programmed experiment. The rate of gas production and product distribution was identical, within experimental error, to the case of KOH/NiO.

The activity of Ni metal adsorbed on graphite was also studied. A temperature-programmed experiment (FIG. 12) showed that Ni metal was active at much lower temperatures than when using NiO-KOH as a catalyst. Arrhenius plots (FIG. 13) showed that the activation energies in the two cases were similar ( $E_a = 25.2 \pm 0.8 \text{ kcal/mol}$  for KOH-NiO and  $E_a = 23.1 \pm 2.6 \text{ kcal/mol}$

for Ni metal), and much lower than in the case of KOH only deposited on graphite ( $E_a = 41.7 \pm 1.3$  kcal/mol). The Ni metal catalyst, however, deactivated rapidly. FIG. 10 (curve B) shows that even though the initial rate of gas production at 859 K was much faster for Ni metal than for NiO-KOH (compare the slopes of curves A and B in FIG. 10), the rate of gas production stops after 10% graphite conversion in the first case (Ni metal), while gas was still being produced after 25% conversion when NiO-KOH was the catalyst.

The results presented show that a mixture of KOH and a transition metal oxide is able to catalyze the gasification of graphite with steam at a detectable rate at temperatures as low as 590 °C. This temperature is 100° lower than the one needed to have a steady-state rate of reaction when KOH alone is used as a catalyst. The KOH-NiO mixture was the most active catalyst found, although other transition metal oxides (especially  $Fe_2O_3$ ) were also effective when codeposited with KOH. The activity of these mixtures as catalyst for the gasification process below 625 °C cannot be attributed to an additive effect, but rather to a cooperative effect. While the mixture of KOH and the transition metal oxide is a good catalyst for the steam gasification of graphite below 625 °C, KOH adsorbed alone behaves as a reactant at this temperature range and the transition metal oxide adsorbed alone is inactive.

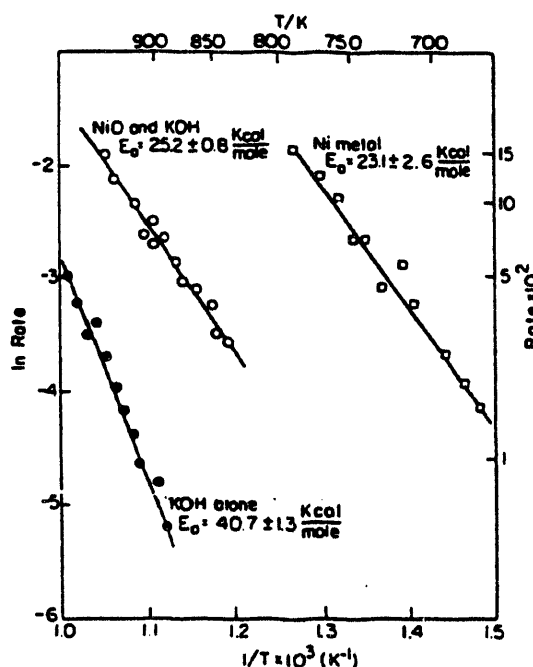


FIG. 13. Arrhenius plots of the temperature dependence of the gas production displayed in FIG. 10 (curves A and B) and in FIG. 12.

In the cases of nickel and iron, even though the oxide adsorbed alone is inactive, the metals are excellent catalysts. The results show that nickel converted to the metallic state when  $\text{Ni}(\text{NO}_3)_2$  was decomposed on graphite in a  $\text{H}_2$  stream at  $800\text{ }^\circ\text{C}$  is an excellent catalyst for this process, while  $\text{NiO}$  produced from decomposition of the same salt at  $400\text{ }^\circ\text{C}$  is completely inactive. Similar results have been found by other authors. MCKEE [10] found that iron is only effective for the gasification of graphite with steam if it is present in the metallic state. WALKER et al. [11] found the same behavior for iron when  $\text{CO}_2$  was used instead of  $\text{H}_2\text{O}$ . YAMADA et al. [12] reported that the activity of nickel compounds in the gasification of char was related to their facility to decompose and produce nickel in the metallic state.

When  $\text{KOH}$  was added to nickel, the temperature at which the nickel nitrate was decomposed did not affect the catalytic activity of the mixture for the gasification of graphite with steam below  $725\text{ }^\circ\text{C}$ . The same activity was found when  $\text{Ni}(\text{NO}_3)_2$  was decomposed at either  $400\text{ }^\circ\text{C}$  or  $800\text{ }^\circ\text{C}$  in the presence of  $\text{KOH}$ . Since at  $400\text{ }^\circ\text{C}$ , the formation of  $\text{Ni}$  metal is not favored, these results suggest that  $\text{KOH}$  is stabilizing the presence of  $\text{NiO}$  at our reaction conditions. This does not exclude, however, that a small fraction of the nickel loading is in the metallic state. FIG. 12 shows that the activation energies of the  $\text{Ni}$  metal and  $\text{KOH-NiO}$  catalysts are very similar, even though the activity of the first is higher. Also, both catalysts show the same product distribution. This is what we would expect if a small fraction of the  $\text{Ni}$  in the  $\text{KOH-NiO}$  catalyst were in the metallic state.

The most important difference between the  $\text{KOH-NiO}$  and the  $\text{Ni}$  metal catalysts is their total activity. FIG. 11 shows that the  $\text{Ni}$  metal catalyst was completely inactive after 11 turnovers (11% graphite conversion) while the  $\text{NiO/KOH}$  catalyst was still active after 25 turnovers (25% graphite conversion). This higher total activity is also found in the case of the  $\text{KOH-Fe}_2\text{O}_3$  catalyst.

The formation of a stable compound by chemical reaction of the transition metal oxide with  $\text{KOH}$  could explain the cooperative effect found in this work. The production of  $\text{K}_2\text{NiO}_2$  and  $\text{FeKO}_2$  from the reaction of  $\text{KOH}$ ,  $\text{K}_2\text{CO}_3$ , or  $\text{K}$  metal with  $\text{NiO}$  or  $\text{Fe}_2\text{O}_3$ , respectively, at temperatures around  $750\text{ K}$  has been reported [13, 14].

The cooperative effect and the high resistance to poisoning clearly show that there is interaction between KOH and the transition metal oxide as catalysts for the gasification of graphite with steam below 625 °C. ADLER and HÜTTINGER have studied the effect of combining  $K_2SO_4$  and  $Fe_2SO_4$  as catalysts for gasification of coke with steam plus hydrogen [15] and have found improvements over the performance of  $K_2SO_4$  alone. A similar situation is found in the industrial steam reforming catalyst, where  $K_2CO_3$  is added to nickel to avoid its poisoning from encapsulation by a carbon layer [16]. On the other hand, WIGMANS and MOULIJN [17] did not find evidence for interaction between  $K_2CO_3$  and Ni metal for the gasification of carbon with steam at 800°C. All this suggests that the interaction between KOH and the transition metal oxide depends on the reaction conditions.

The product distribution obtained for the gasification of graphite with steam when either KOH-NiO or KOH- $Fe_2O_3$  were used as catalysts suggests that the kinetics of a surface reaction is controlling the process. The ratio of CO to  $CO_2$  obtained when either KOH-NiO or KOH- $Fe_2O_3$  is adsorbed on graphite is far below the value expected at equilibrium. Also, the extremely low proportion of  $CH_4$  in the gas products suggests that the process is kinetically controlled. The formation of  $CO_2$  instead of CO has also been found by WIGMANS et al. [18] when Ni metal is used as a catalyst.

The low proportion of  $CH_4$  in the gas products might be due to steam reforming, particularly in the case of nickel, since Ni metal is used as an industrial catalyst for this reaction. Similar results are found, however, in the case of iron compounds which are widely used as a catalyst for the formation of hydrocarbons from  $H_2$  and CO, even in the presence of large concentrations of steam. Another possibility for the low proportion of  $CH_4$  in the gas products is that  $H_2$  is preferentially formed over  $CH_4$  in our reaction conditions. That is, the recombination of hydrogen atoms on the graphite surface is favored over the breaking of a carbon-carbon bond involved in the formation of  $CH_4$  from graphite.

In experiments with K-Ni oxide catalysts, it was found that the catalysts were subject to potential poisoning by sulfur compounds. A search for a more poison-resistant catalyst resulted in finding that calcium-potassium oxide catalysts are almost as active and more poison-resistant than K-NiO catalysts. The poisoning experiments will be described in the section on chars

(SEC. VI-B). TABLE 3 in SEC. VI-B gives a comparison of the activity of several catalysts.

A kinetic study was performed to enhance the comparison between the two most active bimetallic catalysts of those studied for the steam gasification of the various carbon samples investigated. The partial orders of reaction were determined with graphite samples containing a catalyst:carbon molar ratio equal to 0.01 with a mole of catalyst comprising 1 mol of K and 1 mol of Ca or of Ni. The same determination was also made with a K/graphite sample having a catalyst:carbon molar ratio equal to 0.01. One of the reactants ( $H_2O$ ;  $H_2$ ;  $CO_2$ ) was diluted with inert gas (He), while keeping the partial pressure of the other gaseous reactants constant. Every system was kinetically tested after 30% of graphite conversion to ensure that a steady state was achieved (pseudo-zero order). Also, no tests were made after 70% conversion, so that major changes in catalyst:carbon ratio did not affect the final carbon conversion rates. These conditions required selection of different temperatures for each system: K-Ni/graphite, 660° C; K-Ca/graphite, 668 °C; K/graphite, 680 °C.

The high activation energies found for all the carbonaceous and catalyst samples studied in our system along with the very small grain size and the high linear velocity of the gases used indicate that chemical reaction steps are controlling the rate of reaction, and not diffusion.

Most of the kinetic studies reported in the literature have been carried out in gravimetric systems in which the carbon conversion is monitored by weight loss. Because of the characteristics of this reaction (solid-solid and solid-gas reaction), care must be taken to perform kinetic studies in our flow reactor system as shown by HOLSTEIN [24]. We therefore describe below in some detail how we analyzed our data.

During steady-state operation our reactor can be visualized as one in which a constant "flow" of carbon is passing through a stationary catalyst. If all other conditions are constant, including  $H_2O$ ,  $H_2$ , and  $CO_2$  partial pressures, the reaction rate should be constant. This state is experimentally observed with graphite and can be expressed, because of our conditions (low water conversion levels, high space velocity) in a very simplified way, as occurring in a differential reactor. Assuming that the number of moles of catalyst participating in the reaction is constant during the period of investigation, one finds:

$$R_c = (F_o/N_{cat})X \text{ or } R_c = SX,$$

where  $R_c$  is the rate of carbon conversion per mole of catalyst,  $F_o$  is the "molar flow of carbon,"  $N_{cat}$  indicates moles of catalyst in the reactions,  $X$  indicates conversion and  $S$  is the molar space velocity which under our conditions is approximately constant.

The rate expression can be generalized as:

$$R_c = K_f [P^a(\text{H}_2\text{O})P^b(\text{H}_2)\dots].$$

The partial orders of reaction can then be determined by varying the partial pressure of one component while keeping the partial pressures of the other components constant, using an inert gas to maintain the total pressure constant.

Under our conditions,  $\text{CO}_2$  has been shown to have no effect on the reaction rate.

In the presence of a large excess of water or, alternatively, hydrogen, the expression becomes:

$$R_c = K'P^a(\text{H}_2\text{O}) \text{ or } R_c = K''P^b(\text{H}_2).$$

When the experimental data was plotted, good correlations were found, and the orders obtained for every system are presented in TABLE 1.

From these results it is apparent that the inhibiting effect of  $\text{H}_2$  decreases in the order  $\text{K-Ni} > \text{K} > \text{K-Ca}$ . The close values of the

TABLE 1. Steam Gasification of Graphite with Various Catalysts

Catalyst	After 700 min. of reaction under STD conditions		<-----Kinetic Study----->			
	Conversion %	Rate (mol/ mol/min)	$E_a$ (kJ/mol)	$\text{H}_2\text{O}$ partial order (a)	$\text{H}_2$ partial order (b)	Regression (a)-(b)
K-O	15	0.091	265	$0.66 \pm 0.04$	$0.71 \pm 0.01$	0.94-0.99
Ca-O	7	0.040	---	---	---	---
Ni-O	0	0.00	---	---	---	---
K-Ca-O	25	0.139	276	$0.50 \pm 0.03$	$0.21 \pm 0.01$	0.996-0.98
K-Ni-O	28	0.145	273	$0.69 \pm 0.03$	$1.04 \pm 0.01$	0.95-0.99



activation energies indicate that the rate-controlling step may be independent of the catalysts. The high value found (about 60 kcal/mol or 270 kJ/mol) indicates that the rate depends on a thermally activated step such as the surface complex decomposition suggested by MIMS et al. [3].

Water Dissociation with K-Ca-O<sub>x</sub> Catalyst. When steam is passed over the K-Ca-O<sub>x</sub> catalyst in the absence of carbon, the dissociation of water is observed and the evolution of H<sub>2</sub> is readily detectable. The reaction stops after 2 hr at 625 °C when using 0.3g of catalyst and steam at 1 atm. If the temperature is raised, an additional H<sub>2</sub> release is observed, but this always stops after a few minutes at each temperature. No release of O<sub>2</sub> was observed at any time. Blank checks without catalyst showed no H<sub>2</sub> release. H<sub>2</sub> release was observed for one cycle of increasing temperatures only. This is most likely due to the oxidation of the catalyst to a form that is no longer active for water dissociation, as indicated by the absence of oxygen evolution. In the presence of carbon, the water dissociation becomes catalytic, as the carbon provides a sink for the oxygen produced from H<sub>2</sub>O thereby preventing the catalyst deactivation.

### 3) *Mechanism of the Graphite-Catalyst-Steam Interaction.*

In previous sections we reported that mixtures of KOH and various transition metal salts were good catalysts for the steam gasification of graphite and char. These catalysts promote the formation of H<sub>2</sub> and CO<sub>2</sub> above 550°C, and have a high resistance to deactivation. Out of all the catalysts studied, the one derived from a mixture of KOH and Ni(NO<sub>3</sub>)<sub>2</sub> has the best kinetic properties for this reaction. This catalyst, denominated from now on as Ni-K catalyst, shows the highest activity for H<sub>2</sub> production at 580 °C (1.2ml H<sub>2</sub>/min/g carbon) and a relative low activation energy (~30 kcal/mol).

We have used controlled atmosphere electron microscopy (CAEM) to characterize this catalyst in further detail. We studied the interaction between the Ni-K catalyst and graphite surfaces in two gas environments: H<sub>2</sub>O vapor and N<sub>2</sub>/H<sub>2</sub>O. This technique is an excellent tool to study the surface mobility and wetting properties of the catalyst. It also allows the determination of the mode of attack of the gaseous reactants on the graphite lattice, promoted by the catalyst, and the intrinsic rates of carbon consumption. This characteristic is very important because comparisons of the activities of various catalysts can be

made, without the interference of geometric effects, such as surface area or number of active sites.

It has now been shown that the Ni-K catalyst has distinctive morphological and kinetic properties for carbon gasification.

A detailed description of the CAEM technique can be found elsewhere [13]. Ni and K are introduced onto transmission specimens of natural single crystal graphite (Ticonderoga, NY) as an atomized spray, using 0.1% solutions of  $\text{Ni}(\text{NO}_3)_2$  and KOH. Samples were then dried in air and introduced into the environmental cell.

Before the sample was exposed to the reactant gases, it was heated in Ar at 450 °C for 30 min to decompose the  $\text{Ni}(\text{NO}_3)_2$  and achieve a good metal particle nucleation. Particles grew to an average size of 15 nm in diameter.

The gases used—Ar,  $\text{H}_2$ , and  $\text{O}_2$ —were obtained from Scientific Gas Products, Inc., with stated purities of 99.999%, and were used without further purification.  $\text{H}_2$  vapor was introduced into the system by allowing a carrier gas to flow through a bubbler containing deionized  $\text{H}_2\text{O}$  at 20 °C. This procedure produces a gas: $\text{H}_2\text{O}$  ratio of ~40:1 in the gas reaction cell.

After graphite samples loaded with KOH and  $\text{Ni}(\text{NO}_3)_2$  were treated at 450 °C in Ar, particle nucleation was observed on both the basal and the edge planes. When the sample was treated in a water vapor environment (2 Torr Ar: $\text{H}_2\text{O}$ , 40:1), the particles located on the graphite edge region underwent a transformation from nonwetting condition to wetting condition between 475 and 525 °C. They spread over the whole edge area and formed a very thin film that became very difficult to observe. This suggests that the film width is of the order of the apparatus resolution (2.5 nm).

On continued heating to 555 °C these regions started to erode, giving a ragged appearance to the initially uniform edges. The carbon erosion developed into a more ordered edge recession as the temperature approached 675 °C. FIGS. 14A and 14B show a two-picture sequence illustrating this mode of attack. The interval between A and B is 3 sec at 900°.

The edge recession involved the whole area and the various fronts of attack were separated by 60° angles, in the direction parallel to the 1120 crystallographic orientation of the graphite

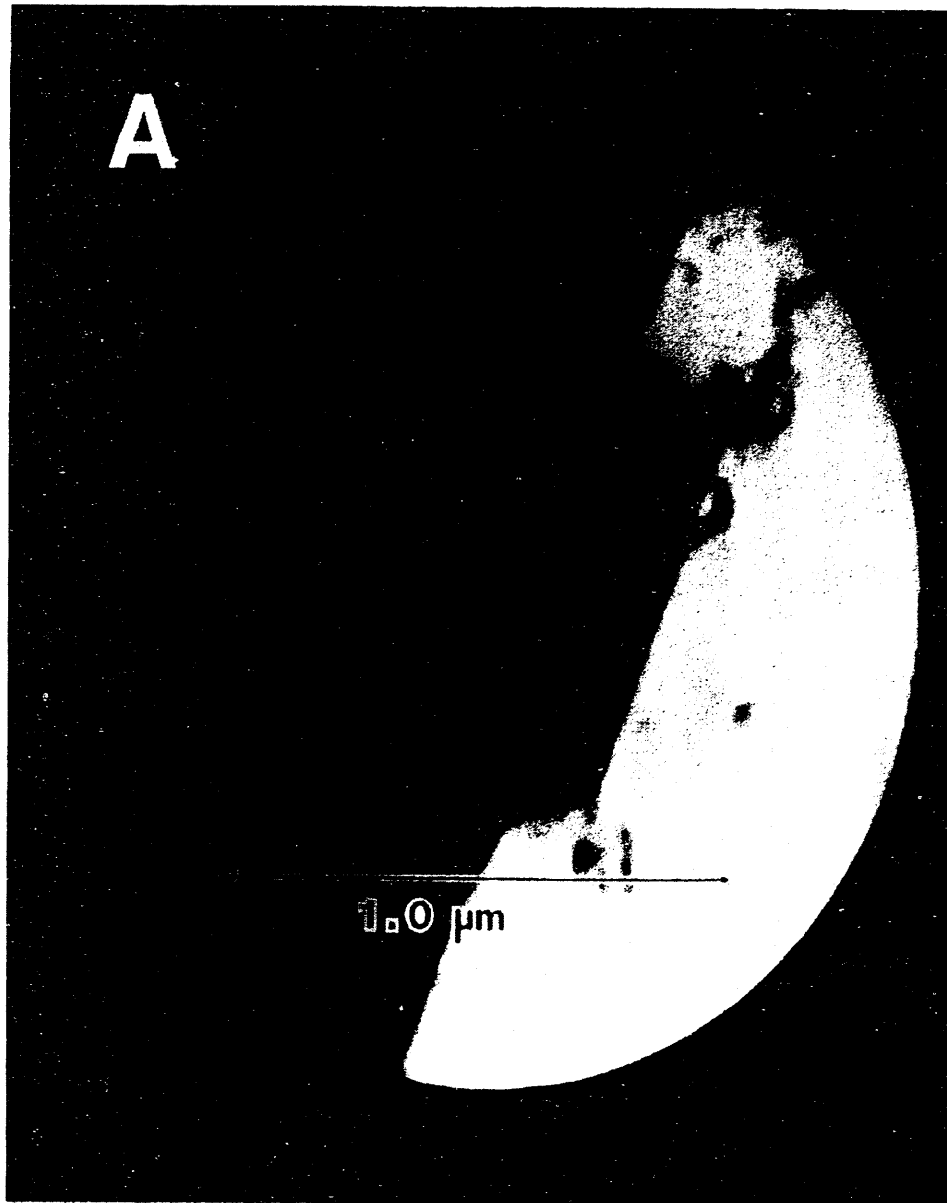


FIG. 14. Sequence of photographs taken from the CAEM video display, showing the edge recession attack of carbon in H<sub>2</sub>O vapor at 900 °C. The time between (a) and (b) is 3 sec. XBB 867-5379B

structure. The orientation was determined by referring the position of the fronts of attack to that of twin bands, which are always present in the graphite in the 1010 direction.

The rate of edge recession increased continuously when the temperature was raised from 675 to 1100 °C, and no evidence of deactivation was observed. A quantitative analysis of the rates of edge recession as a function of temperature is shown in FIG. 15 in the form of an Arrhenius plot. An activation energy of  $30.8 \pm 0.9$  kcal/mol was obtained. This value is consistent with the one obtained from kinetic studies using a flow reactor system.

At temperatures above 955 °C, a change in the mode of attack was observed. The film responsible for the edge recession sintered into small particles that promoted the formation of channels. This phenomenon may be caused by a change in the characteristics of the catalyst brought about by a buildup of H<sub>2</sub> produced in the gas environment. This is in agreement with the results described in the following paragraphs.

The catalytic effect of Ni/K mixtures on the gasification of graphite on a H<sub>2</sub>:H<sub>2</sub>O 40:1 atmosphere was studied on samples that had been either gasified in steam at 1000 °C or heat-treated in Ar at 450 °C. The results in both cases were identical, and they will be described without making reference to the sample pretreatment.

The first signs of catalytic attack when the specimens were heated at 2.0 Torr wet H<sub>2</sub>O were observed at 545 °C. It took the form of relatively straight channels which were created by catalyst particles that had nucleated along the edges of graphite.

When first formed, the channels remained parallel-sided, and as the temperature was raised to 565 °C, they started to acquire a fluted appearance. This is the result of active catalyst particles spreading along the channel walls, which then proceeded to catalyze the reaction by an edge recession mode. (See region indicated by arrows in FIGS. 16A and 16B).

On raising the temperature to 675 °C, many of the previously inactive particles located on the graphite basal plane started to exhibit mobility. When these particles encountered an edge, they underwent a rapid spreading action and this resulted in a subsequent removal of carbon by edge recession in directions parallel to the 1120 crystallographic orientation. The variation

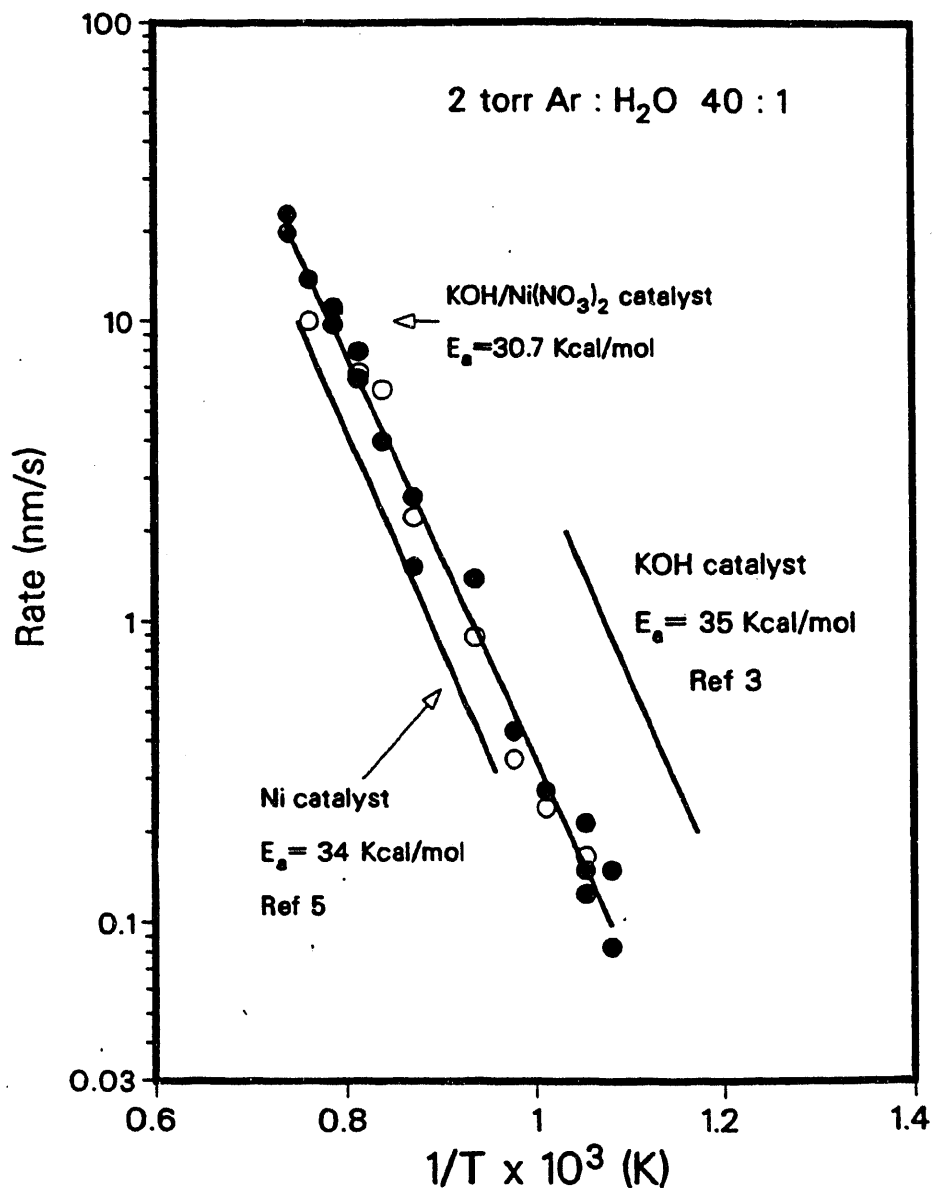


FIG. 15. Arrhenius plot of Ni/K catalyzed edge recession rates of graphite in 2 torr of wet Ar. The filled circles represent the results obtained after heat treating the sample in Ar for 30 min at 450 °C. The open circles represent the results obtained after treating the sample in 2 torr of wet H<sub>2</sub> at 1100 °C. Results previously reported for KOH and Ni metal are included for comparison purposes. The length of the curves indicates the temperature range studied. XBL 873-1273

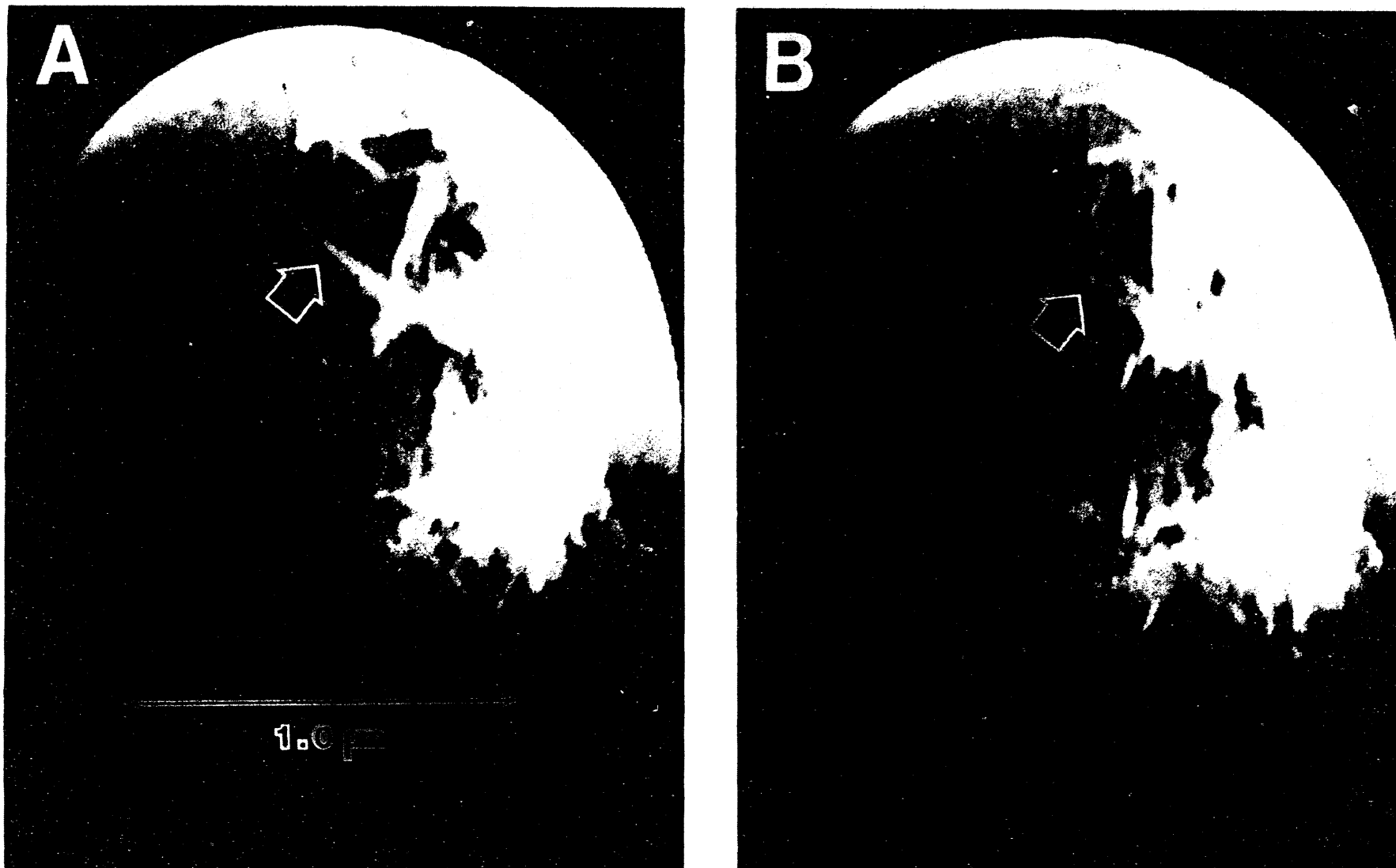


FIG. 16. Sequence of photographs, showing the modes of attack in 2 torr of wet  $H_2$ . The region indicated by the arrows shows the recession of the channel walls, as described in the text (see Results). Also note the simultaneous carbon attack by edge recession and channeling in the lower part of the photographs. The time between (a) and (b) is 1 sec. XBB 871-50B

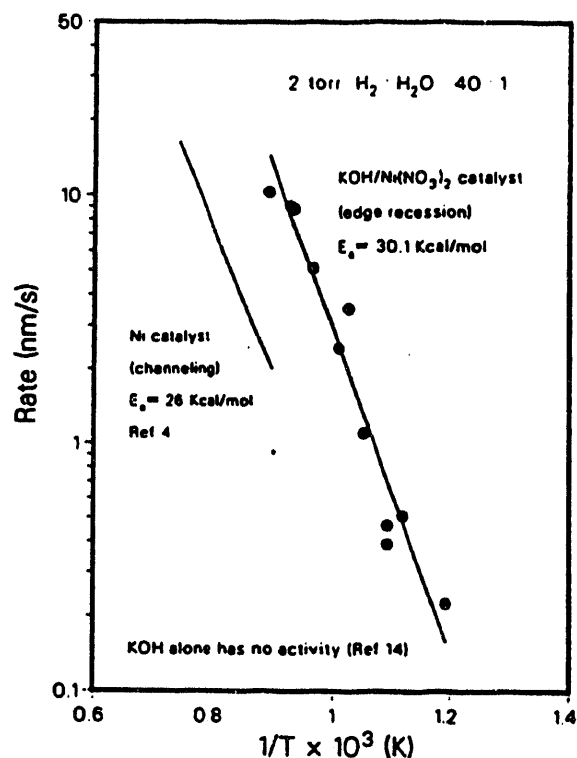


FIG. 17. Arrhenius plot of Ni/K catalyzed edge recession rates of graphite in 2 torr of wet  $H_2$ . The results previously obtained for the channeling mode of attack of Ni metal are included for comparison. The length of the curves indicates the temperature range studied. XBL 873-1271

in edge recession rate with temperature was determined and the data are presented in FIG. 17 in the form of an Arrhenius plot. An activation energy of  $30 \pm 2$  kcal/mol was obtained from the slope of this line.

Both modes of attack, edge recession and channeling, were occurring simultaneously during the whole temperature range studied (600-1100 °C). Below 900 °C the channels were very short and were usually taken over by the progress of the recession of neighbor edges. As the temperature was raised to 1100 °C the edge recession tended to slow down and in some regions it stopped completely, leaving channeling as the only mode of attack.

The edge recession activity could be regenerated by treating the sample in wet Ar at about 1000 °C. The wet  $H_2$  treatment did not affect the properties of the Ni/K mixture for promotion of the edge recession mode of attack of steam. FIG. 15 shows that the rates of edge recession obtained in wet Ar after a  $H_2/H_2O$

treatment (open circles), are identical to those obtained after a heat treatment in Ar (filled circles).

The Ni/K mixture catalyzes the gasification of graphite in both reducing and oxidizing environments. The carbon consumption in all cases occurs at the catalyst/carbon interface and the gas mode of attack is affected by the morphology of the mixture on the surface. In wet Ar, the catalyst spreads and promotes the carbon attack by an edge recession mode. In wet H<sub>2</sub>, the catalyst is present in both a wetting and a spreading condition, and the gasification occurs simultaneously by channeling and edge recession.

The surface tension forces among the carbon substrate (solid), the catalyst (liquid), and the gas environment control the wetting properties of the catalyst, and are responsible for the different modes of attack observed. The catalyst spreads over the carbon surface, and favors edge recession, because the sum of the surface tensions at the catalyst-substrate ( $\gamma_{sl}$ ) plus catalyst-gas ( $\gamma_{lg}$ ) interfaces is lower than the surface tension at the gas-substrate interface ( $\gamma_{sg}$ ):

$$\gamma_{sg} > \gamma_{lg} + \gamma_{sl}$$

This is the case in H<sub>2</sub>O vapor and O<sub>2</sub>/H<sub>2</sub>O environments, but there are differences in catalyst behavior between these two cases. In wet O<sub>2</sub>, at 500 °C, the catalyst forms particles that only wet the carbon surface and, as the temperature rises above 650 °C, these particles spread over the edge planes. In wet Ar the opposite behavior is observed. The catalyst spreads at temperatures as low as 500 °C and, as the temperature approaches 1000 °C, particle nucleation takes place.

CAEM experiments were also carried out during steam gasification of graphite impregnated with K-Ca oxide catalysts. The results, details of which are shown in reference [25], essentially confirm and duplicate the findings with K-Ni oxide catalysts.

It has previously been stated that the mechanism of steam gasification of carbonaceous materials involves a dissociation of water, with H<sub>2</sub> going into the gas phase and O<sub>2</sub> forming oxygenated compounds on the carbon surface. This is indicated in FIG. 18 which shows the H<sub>2</sub>/CO<sub>2</sub> ratio produced during gasification. Initially this ratio is more than 2, while O<sub>2</sub> is adsorbed on the carbon. At the end of gasification, the ratio drops below 2 as dissociation of oxygenated carbon accelerates.



Elucidation of the structure and stability of the various surface species formed after adsorption of  $O_2$ ,  $CO_2$ ,  $H_2$ , and  $H_2O$  on graphite is very important for the understanding of the chemistry of graphite, and its connection with processes leading to the stabilization of high surface area carbons or to carbon gasification. Although numerous studies have focused on the kinetic properties and the nature of the surface species formed after  $O_2$ ,  $H_2O$  or  $CO_2$  oxidation, only a limited understanding has yet been achieved, owing certainly to the complexity of the system.

TPD and XPS studies of  $O_2$ ,  $CO_2$  and  $H_2O$  adsorption of clean polycrystalline graphite were performed [20]. They showed the presence of semi-quinones and lactones on the graphite surface after  $CO_2$  adsorption.

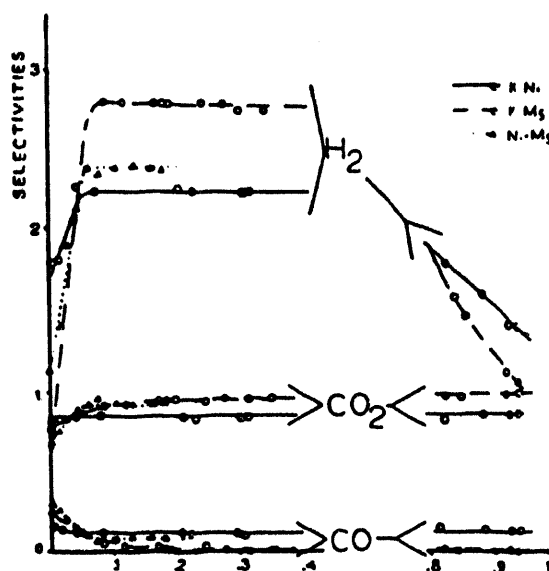


FIG. 18.  $H_2$  and  $CO_2$  selectivity during gasification [19].  
LBL-27175

## B) Steam Gasification of Chars

### 1) Potassium-Nickel Oxide Catalysts.

The gasification rates of five different chars have been obtained. The chars' pre-treatment, elemental composition and ASTM rank are summarized in TABLE 2. Nickel and potassium were loaded on the carbon substrate by the incipient wetness method using solutions of  $\text{Ni}(\text{NO}_3)_2$  and  $\text{KOH}$ . A detailed explanation of the sample treatment after catalyst loading is given in a publication [20] and in an earlier section of this report.

A detailed explanation of the equipment used in these studies is given in SEC. V-A. The kinetic studies were done in a fixed bed flow reactor with an online gas chromatograph used for product analysis. The total gas production as a function of time was determined using a gas burette after the steam was condensed. The XPS study was done in an Ultra-High Vacuum (UHV) chamber coupled to a high pressure cell. This apparatus

TABLE 2. Characteristics of Coal Char and Graphite Samples Used in This Study

Name	ASTM Rank <sup>a</sup>	Pretreatment	←-----Analysis (wt %) <sup>b</sup> ----->					
			C	H	N	O	S <sup>c</sup>	Ash <sup>d</sup>
Western Kentucky Washed (WK)	NV.B. Bit.	Unspecified	72.3	3.2	1.4	7.9	3.2	12
North Dakota Husky (NDHL)	Lignite	Partial steam gasification	71.2	1.1	0.37	13-17	2.0	8-12 <sup>e</sup>
Montana (MS)	Subbituminous	Partial steam gasification: T = 1200K	66.0	1.1	0.20	---	0.92	---
Illinois #6 High Temp. (I6HT)	HV.C.Bit.	Heated under He: T = 1300K	---	---	---	---	---	---
Illinois #6 Low Temp. (I6LT)	HV.C.Bit.	Pregasifier Heater: T = 670K	72.0	3.3	1.5	10.9	2.6	9.1
Graphite UCP-2	---	None	100	0	0	0	0	0

<sup>a</sup>HV = High volatility B and C indicate bituminous classes.

<sup>b</sup>Dry mineral matter containing basis. Oxygen by difference.

<sup>c</sup>Total sulfur.

<sup>d</sup>By low temperature technique (oxygen plasma).

<sup>e</sup>Not measured. Range of values reported in [12].

Source of chars: I.G.T.

allowed us to treat the sample under reaction conditions and to further transfer it to UHV for surface characterization without exposure to air.

All the kinetic results were obtained in isothermal experiments. The steam flow through the sample was equivalent to 1 ml of liquid water per minute. The reactor diameter was 0.6 cm. The reaction temperature was measured using a chromel-alumel thermocouple in contact with the external wall of the reactor. At the beginning of each experiment, a stabilization period of 15 min was allowed before data was collected. The principal reaction products were  $H_2$  and  $CO_2$ . The gasification rates were determined by measuring the  $H_2$  production because its solubility in water is much smaller than that of  $CO_2$ . The carbon conversions were determined by dividing the number of  $H_2$  moles produced by two times the initial number of carbon moles.

The XPS experiments were carried out using a Mg-anode source ( $h\nu = 1253.6$  eV). The data were collected using a detector pass energy equal to 40eV. The position of the peaks was calibrated with respect to the position of the  $C_{1s}$  peak of graphite (binding energy = 284.6eV).

The rate of gasification of several chars with steam was studied as a function of time in the presence of a 1:1 mixture of nickel and potassium oxides. A description of the five chars studied is given in TABLE 1. For all of them, the steady state rate after 1.0 hour is at least one order of magnitude higher than that of graphite (see FIG. 19a). This is reflected in a much higher carbon conversion after 6.0 hours (see FIG. 19b), even though by then, the char steam gasification rates have decreased to values similar to those of graphite.

A comparison of the gasification rates for a 1:1 mixture of potassium and nickel oxides with that of the components deposited alone is given in FIGS. 20a and 20b for two of the chars studied (Illinois #6 High Temp. and Montana). In the case of the Illinois #6 char, it is clear that the mixture is more active than the sum of the rates of the components deposited alone. (Compare Curves A and D in FIG. 20a). In contrast to the results obtained with graphite, the mixture in this case is more than two times as active as nickel deposited alone. For the Montana subbituminous char, the rate of gasification of the mixture is similar to that of nickel alone and higher than that of potassium (see FIG. 20b).

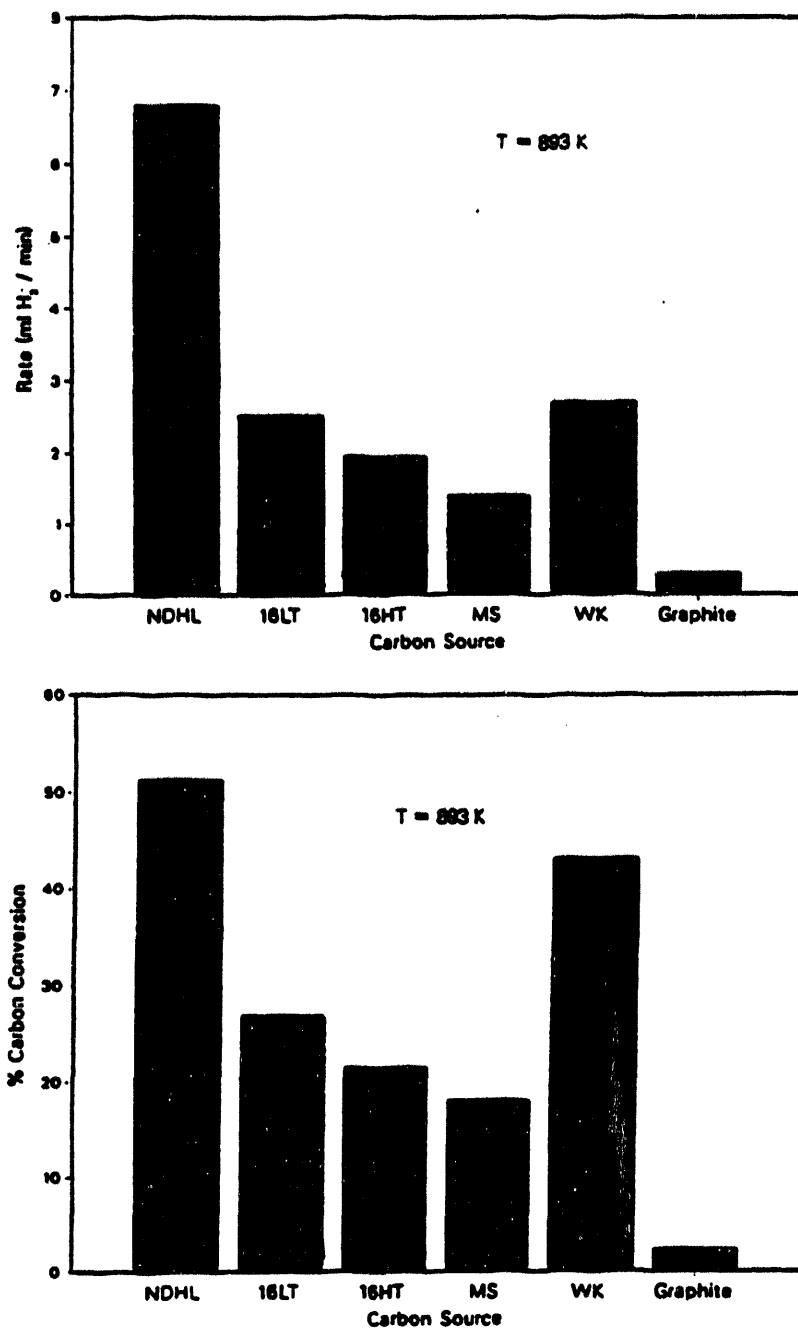
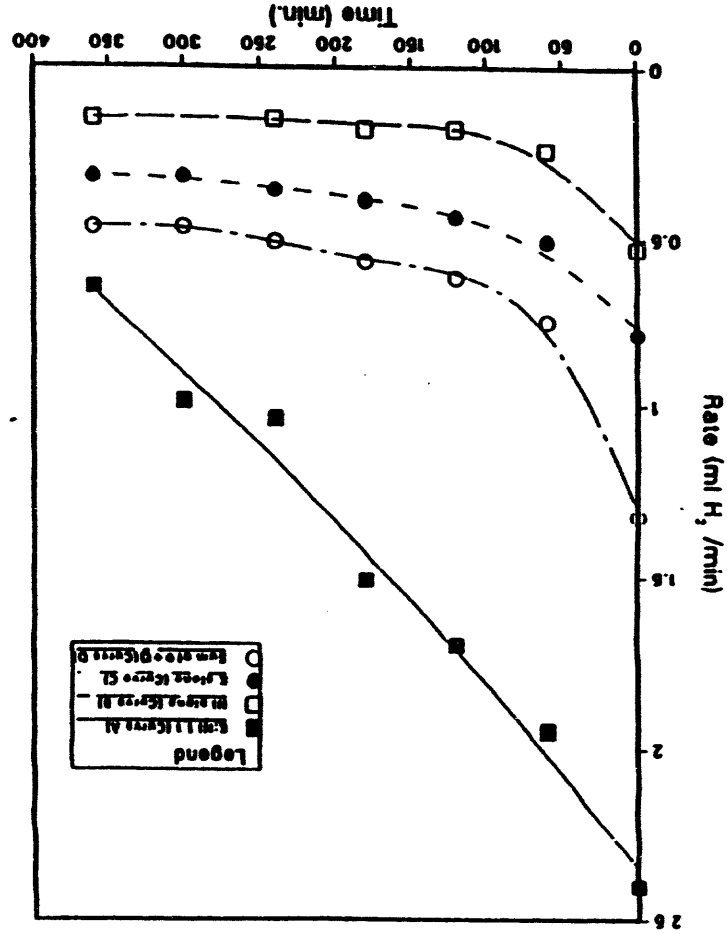
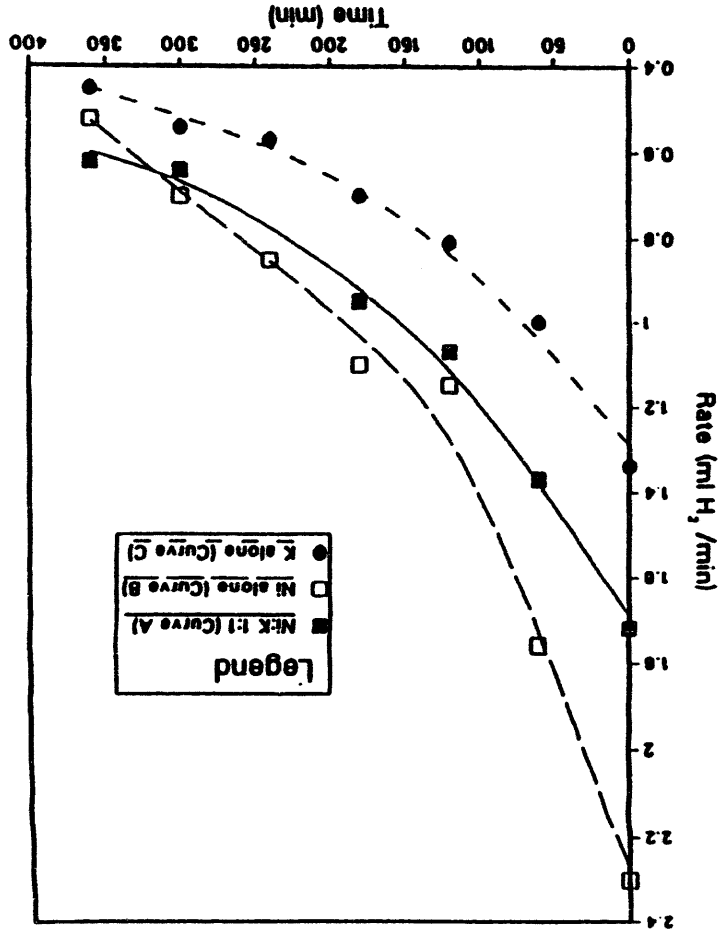


FIG. 19. (a) Steady state steam gasification rates of several carbonaceous solids after 1.0 hour when a mixture of nickel and potassium oxides is used as a catalyst. (b) Percentage of carbon conversion obtained after 6.0 hours when the same catalyst is used.

A surface science study of the interaction of potassium, nickel and carbon in the presence of water has been done. XPS of the  $\text{Ni}_{2p_{3/2}}$  signal of two systems, a 1:1 Ni:K mixture codeposited on graphite and nickel deposited alone, have been obtained after exposing them to 24 torr of water vapor at 950K. The ki-

FIG. 20. Steam gasification rates at 893K for two chars, (a) Illinois No. 6 High Temp. and (b) Montana, catalyzed by three different compounds, a 1:1 mixture of nickel and potassium (curve A), nickel alone (curve B) and potassium alone (curve C). In FIG. 20a, curve D is the mathematical sum of curves B and C



netic results show that at this temperature both systems are catalytically active. FIG. 21 (Curve A) shows the spectrum corresponding to nickel deposited alone. There is a peak at 855.2 eV with a small satellite peak at 862.7 eV. This is characteristic of nickel in the metallic state and agrees with results obtained by us for nickel foil. The shoulder at 857.5 eV is due to small amounts of NiO in the sample. When nickel and potassium are codeposited on graphite (Curve B in FIG. 21) the binding energy of the Ni<sub>2p<sub>3/2</sub></sub> XPS peak is at 856.4 eV. This indicates that nickel is present in its +2 oxidation state. The much larger satellite peak at 864.6 eV also shows that nickel forms an oxide at this temperature in the presence of potassium. The lower binding energy of the Ni<sub>2p<sub>3/2</sub></sub> peak in the nickel-potassium mixture compared to NiO shows that there is an electronic interaction between nickel and potassium.

The kinetic results presented here indicate that mixtures of potassium and nickel oxides are good catalysts for the gasification of carbonaceous solids with steam. The high reaction rates and carbon conversions obtained with the several chars studied (FIGS. 19 and 20) and the graphite gasification activity after 400 hours support this conclusion.

We previously concluded that there is a cooperative effect between potassium and nickel in this catalyst. The results shown here present the clearest evidence obtained so far for this effect. In FIG. 19a the gasification rate of the Illinois #6 char in the presence of the mixed catalyst is higher than that of the mathematical sum of the rates of the components deposited alone. The XPS results in FIG. 21 show that nickel deposited alone is active as a gasification catalyst when it is present in the metallic state, while in the nickel-potassium mixture, the nickel is catalytically active being in the +2 oxidation state. Also, the shift to lower binding energies for the Ni<sub>2p<sub>3/2</sub></sub> peak in the potassium-nickel catalyst when compared to the position of the NiO peak is evidence for chemical interaction between nickel and potassium. We propose that this synergistic effect is due to the formation of a mixed oxide (K<sub>x</sub>Ni<sub>y</sub>O) that is not readily reduced by carbon under our reaction conditions (<725 °C). There is evidence in the literature for the presence of several nickel-potassium mixed oxides [22], but we do not have enough information to decide which of them is present in our system.

Mixtures of transition metals and alkaline metals as catalysts for steam gasification of various carbon sources have been re-

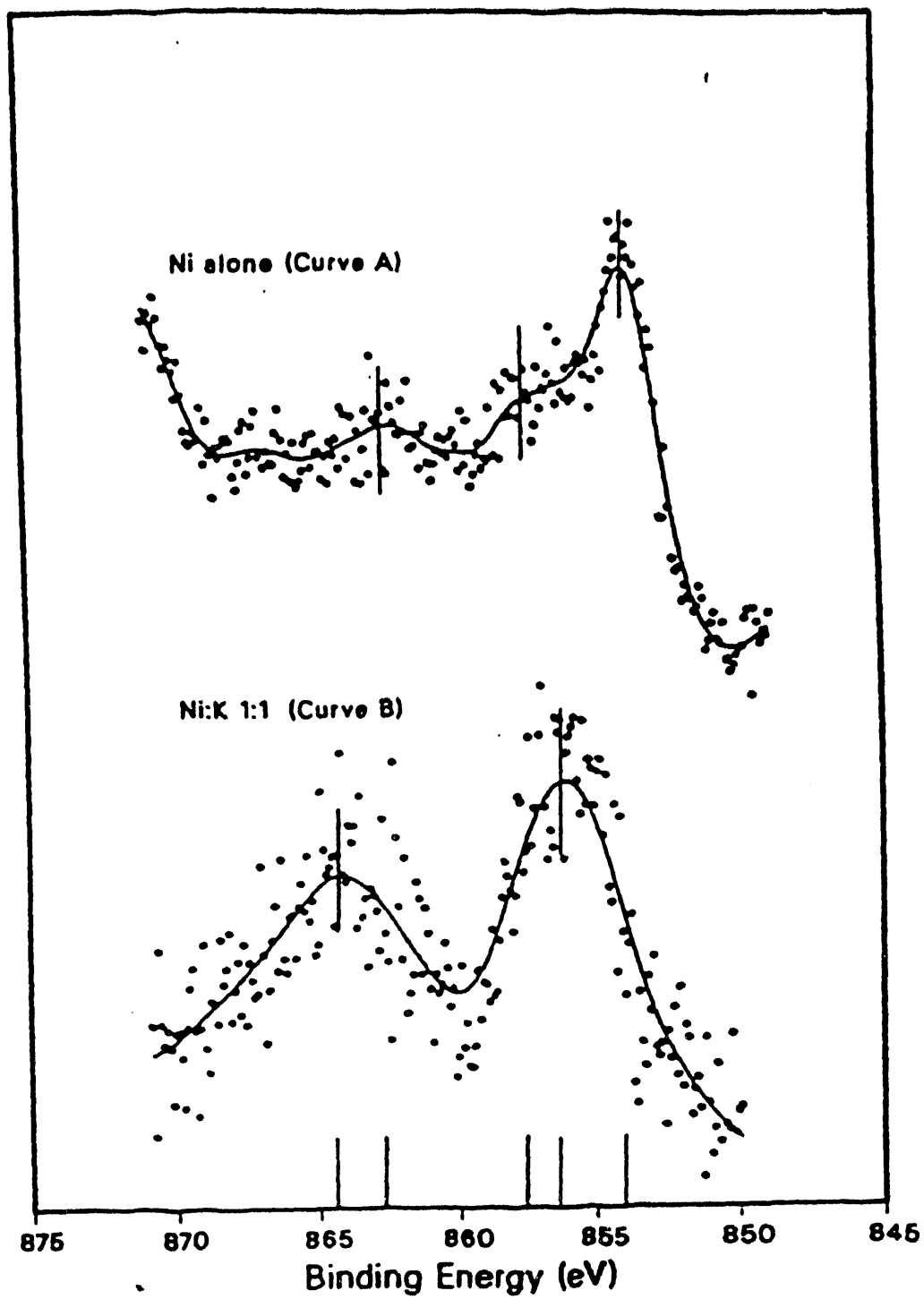


FIG. 21.  $\text{Ni}_{2p_{3/2}}$  XPS of nickel (curve A) and a 1:1 Ni:K mixture (curve B) deposited on graphite. The spectra was taken after exposing the samples to 24 torr of water at 923K for 15 min.

ported previously. WIGMANS and MOULIJN [17] reported that there was no interaction between nickel and  $K_2CO_3$  for the steam gasification of chars at 750 °C. Similar results were obtained in our laboratory when the gasification of graphite was studied above 725 °C. Also, XPS data obtained in our laboratory show that at 725 °C the nickel is present in the metallic state, even in the presence of potassium. We suggest that these results are due to the decomposition of this mixed oxide and reduction of the nickel by carbon. In contrast with the results reported by WIGMANS and MOULIJN, a cooperative effect between a transition metal and an alkaline metal has been reported by two other authors. ADLER and HÜTTINGER [15] found that mixtures of  $FeSO_4$  and  $K_2SO_4$  deposited on PVC coke were better catalysts than the salts deposited alone. Also, SUZUKI et al. [23] reported that  $Na(HFe(CO)_4)$  is a good catalyst for the gasification of various coals with steam. They suggest that this high activity is due to the interaction between iron and sodium.

## 2) *Potassium-Calcium Oxide Catalysts.*

We have earlier described research using only potassium oxide as a catalyst for gasification. We also found that potassium-nickel oxide mixtures exhibited markedly higher activity than that of either  $K_2O$  or  $NiO$  [13]. In the following, we describe the behavior of a superior poison-resistant catalyst mixture, potassium-calcium oxide, for the steam gasification of carbon solids. This catalyst exhibits high activity at relatively low temperatures (575-625 °C) and it produces primarily  $H_2$  and  $CO_2$ . The activity is at least partially attributable to the excellent wetting of carbon by the catalyst precursors in their molten state prior to their decomposition.

Electron microscopy studies indicate that a homogeneous binary catalyst is formed after decomposition of the nitrate precursor salts and that gasification occurs by edge recession of the graphite prismatic planes while the basal plane is unreactive. This is similar to findings with  $K-Ni-O_x$  catalysts. Water dissociation by the  $K-Ca-O_x$  catalyst was found to be an important reaction step. Hydrogen is released and oxygen forms compounds with the carbon. The rate-limiting step appears to be the breaking of C-C bonds releasing carbon oxides.

Chars contain C-H bonds in addition to C-C bonds and have much higher surface areas than graphite. Since both the H/C



TABLE 3. Steam Gasification of Graphite with Various Catalysts

Catalyst	After 700 min. of reaction under STD conditions	
	Conversion %	Rate (mol/ mol/min)
K-O	15	0.091
Ca-O	7	0.040
Ni-O	0	0.00
K-Ca-O	25	0.139
K-Ni-O	28	0.145

ratio and the surface area (as well as mineral impurities content) vary from char to char, several different char types were investigated to establish the catalyst performance for their steam gasification. In TABLE 3, data for the K-Ca-O<sub>x</sub> catalyzed gasification of various chars are compared. The activation energies are similar to that of graphite, indicating that the much higher conversion and rates compared to those of graphite must be due to the char composition. The rate of gasification proceeds in the order, lignite > subbituminous > bituminous > graphite. It should be noted that K-Ni-O<sub>x</sub> exhibited identical trends when different chars were compared with graphite. Thus, the observed rate data is not a unique property of the K-Ca-O<sub>x</sub> catalyst. The chars contain hydrocarbons that appear to gasify more rapidly than graphite. The reaction of steam with C-H bonds is more facile than the reaction with C-C bonds. In no case were hydrocarbons observed in the reaction products.

It was found that the K-Ca-O<sub>x</sub> catalyst is highly resistant to poisoning by the sulfur content in the char. When K-Ni-O<sub>x</sub> catalyst was used for steam gasification, it was rapidly poisoned in the presence of sulfur.

FIG. 22 compares the rates of steam gasification under the standard conditions of a demineralized char loaded with either K-Ca-O<sub>x</sub> or K-Ni-O<sub>x</sub> in the presence or absence of 3% sulfur (obtained by the decomposition of dibenzothiophene) to demonstrate the poison-resistant behavior exhibited by the K-Ca-O<sub>x</sub> catalyst.

The K-Ca-O<sub>x</sub> catalyst is much more active than potassium oxide or calcium oxide alone as shown in TABLE 3. Its reaction rate is twice that of K-O<sub>x</sub> and fivefold that of Ca-O<sub>x</sub> at a

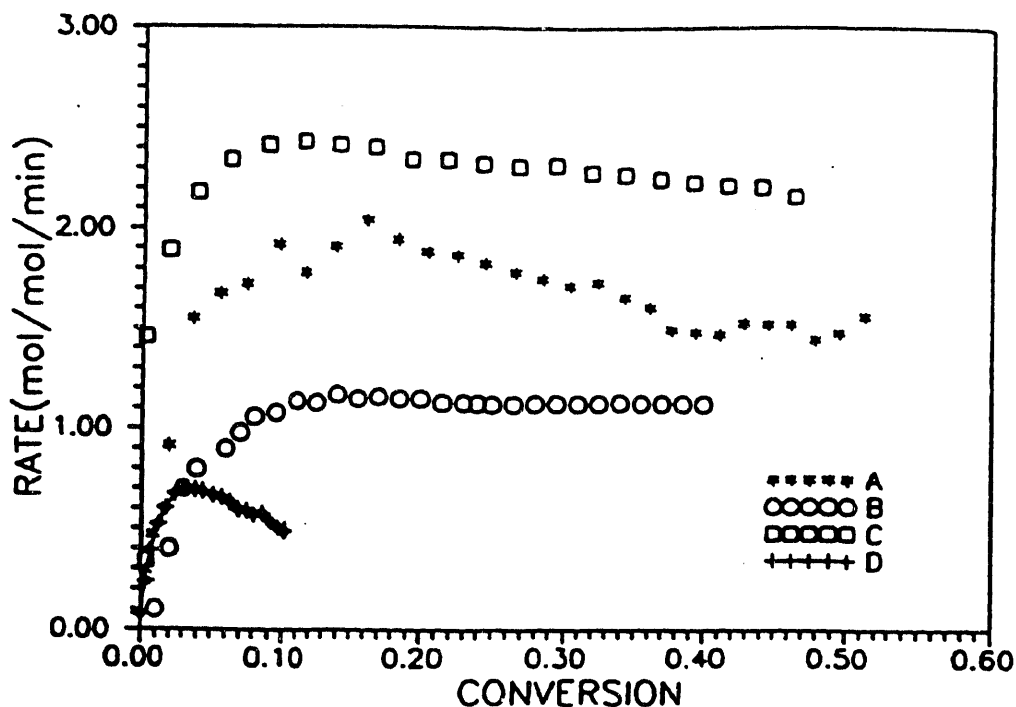


FIG. 22. Sulfur poisoning of demineralized K-Ni/KY 13 char and K-Ca/KY 13 char systems. Rate *vs.* conversion plots. (a) K-Ca/KY 13 char; (b) K-Ca/KY 13 char + 3% S (ex DBT); (c) K-Ni/KY 13 char; and (d) K-Ni/KY 13 char + 3% S (ex DBT).

temperature of 620 °C and 750 torr of steam. This high activity is probably due to the inhibition of a stable calcium carbonate formation that results in the case of calcium alone as a catalyst. In addition, the formation of a molten eutectic phase which is observed during the catalyst preparation and prior to decomposition of the nitrate salts provides good wetting of the carbon solids.

Much of the work carried out with chars was with three chars, a subbituminous (Rosebud) and two bituminous chars (OH Pitt #8 and KY 13) supplied by IGT. Analysis of these is shown in TABLE 4.

The rate equation for the gasification reaction and the activation energies for gasifying the various carbon solids (graphite and different chars) are very similar for different catalysts although the hydrogen inhibition effect varies somewhat from catalyst to catalyst, being the smallest for the K-Ca-O<sub>x</sub> catalyst. Several oxygenated carbon species can coexist at the temperature range used in this work. However, the decomposition temperature for each of these species is different and the type of carbon oxide released can be different. Phenolic species decompose at temperatures higher than those used here and

TABLE 4. Proximate, Ultimate and Inorganic Chemical Analyses of Coals Used in Gasification Tests (data supplied by I.G.T.)

Seam	OH Pitt No. 8					
Mine	Rosebud	Franklin 125	KY No. 13			
<i>Proximate Analysis, wt %</i>						
Moisture	23.1	2.5	9.8			
Volatile Matter	28.5	38.6	32.2			
Ash	11.3	7.5	7.3			
Fixed Carbon	37.1	51.4	50.7			
TOTAL	100.0	100.0	100.0			
<i>Ultimate Analysis, wt % (dry basis)</i>						
Ash	14.66	7.68	8.08			
Carbon	62.78	74.47	73.74			
Hydrogen	4.40	5.24	4.82			
Sulfur	1.29	3.21	1.40			
Nitrogen	0.99	1.50	1.85			
Oxygen (by difference)	15.88	7.90	10.11			
TOTAL	100.00	100.00	100.00			
<i>Ash Composition, wt %</i>						
SiO <sub>2</sub>	48.8	41.6	58.5			
Al <sub>2</sub> O <sub>3</sub>	23.55	20.9	26.9			
Fe <sub>2</sub> O <sub>3</sub>	7.02	31.7	8.1			
TiO <sub>2</sub>	0.12	1.02	0.87			
P <sub>2</sub> O <sub>5</sub>	0.25	0.07	0.16			
CaO	7.16	1.14	0.90			
MgO	2.57	0.36	1.21			
Na <sub>2</sub> O	0.09	0.35	0.24			
K <sub>2</sub> O	0.36	0.98	2.94			
SO <sub>3</sub>	9.91	1.00	0.80			
TOTAL	99.78	99.2	100.62			
<i>Ash Content (as ashed for analysis of ash, dry basis)</i>						
	11.1	7.7	8.2			
<i>Basic Ash Constituents, wt %</i>						
	19.22	35.2	13.4			
<i>Dolomite Ratio, wt %</i>						
	56.6	4.3	15.8			
<i>SiO<sub>2</sub>/Al<sub>2</sub>O<sub>3</sub> Ratio</i>						
	2.1	2.0	2.2			
<i>Forms of Sulfur, wt % (dry basis)</i>						
Pyritic	0.76	2.37	0.40			
Sulfate	0.015	0.21	0.10			
Organic	0.52	0.97	1.03			
TOTAL	1.28	3.56	1.53			
<i>Forms of Iron (dry basis)</i>						
	wt %	% of Fe	wt %	% of Fe	wt %	% of Fe
Pyritic	1.32	62*	2.07	96	0.35	70
HCl-soluble	0.12	6	0.08	4	0.15	30
TOTAL	2.13*	100	2.15	100	0.50	100
Acid-insoluble	0.69	—	<0.10	—	<0.1	—
<i>Pyritic, % of total Fe**</i>						
	—	97	54			

\*Based on total iron, including 0.69 wt % HCl-insoluble

\*\*Of 1/4-inch-top size coal after storage

produce predominantly CO rather than CO<sub>2</sub>. Under our conditions, carboxylates and lactone species are decomposed, producing CO<sub>2</sub> [20].

It appears that the mechanism of gasification is very similar for the three catalysts. As suggested by earlier studies [8, 12], the C-C bond breaking next to a surface carbon-oxygen complex to produce CO<sub>2</sub> (or CO at higher temperatures) is the likely rate-determining step for carbon gasification. There is a great deal of supporting evidence for this model, including oxygen- and carbon-labeled isotope studies and temperature-programmed thermal desorption [8, 12]. The formation of stable oxygenated surface species has been identified by spectroscopic techniques such as EPR, FTIR, and XPS [26]. Also, the change in H<sub>2</sub>/CO<sub>2</sub> ratio during steam gasification clearly indicates oxygen uptake by carbon in the beginning of the reaction [19].

The dissociation of water into hydrogen and oxygen by the catalyst has also been identified as an important reaction step. Surface science studies [27, 28] have shown the ability of potassium to dissociate water to produce K-O<sub>x</sub>. It appears that the evolution of hydrogen derives from this process, as does the oxidation of carbon at the catalyst interface. Our results show that water dissociates by a stoichiometric reaction over the K-Ca-O<sub>x</sub> catalyst. In the presence of carbon, this reaction becomes catalytic and is an important step in the gasification although its activation energy is relatively low (138 kJ/mol or 33 kcal/mol of H<sub>2</sub>) [21].

Chars gasify at much higher rates than graphite (over tenfold increase, TABLE 5). It is clear that gasification of the carbons that contain many C-H bonds in addition to C-C bonds is more facile. This has the effect of increasing the rate without change in the activation energy for the process. Thus, it appears that the rate of gasification is the same for graphite and for chars, but that the preexponential factor is greatly increased for chars. This could be related to the much higher edge density of chars. These are the sites from which gasification proceeds.

The K-Ca-O<sub>x</sub> catalyst exhibits superior poison resistance compared to that of the K-Ni-O<sub>x</sub> catalyst, which has similar steam gasification activity. This property should be of importance in the technology as it permits the use of carbon feedstocks that have not been demineralized or contain sulfur.

TABLE 5. Steam Gasification of Three Chars and of Graphite with K-Ca-O Catalysts

Char (rank)	Activation Energy (kJ/mol)	% Conversion After 120 min Reaction	Reaction Rate (mol/mol/min) 120 min
Graphite	260	10	0.6
North Dakota (lignite)	234	45	15.6
Rosebud (subbituminous)	240	30	2.75
KY 13 (bituminous)	269	15	0.82

A comparison of the K-Ca oxide and K-Ni oxide catalysts is shown in FIG. 23 for the subbituminous Rosebud char. It shows higher activity for the K-Ca oxide catalyst. When the chars were first demineralized by HCl-HF treatment, the K-Ni oxide performed better than the K-Ca oxide and better than the non-demineralized char with K-Ni oxide. The demineralization apparently removed components in the ash which promoted the K-Ca oxide. It also removed components in the ash which promoted the K-Ca oxide.

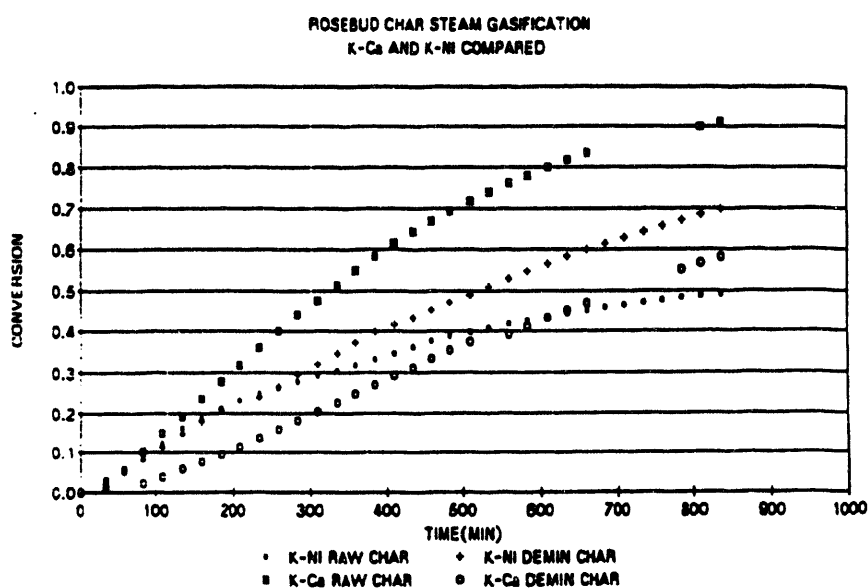


FIG. 23. Comparison of calcium-potassium oxide and nickel-potassium oxide catalysts for steam gasification of subbituminous (Rosebud) char.

Using the K-Ca oxide catalyst for different chars, it is apparent that the subbituminous Rosebud char gasifies better than the two bituminous chars tested (FIG. 24). The bituminous chars after demineralization performed somewhat better than the raw chars, while the reverse was true for the subbituminous char.

A similar picture evolves from the activation energies of the K-Ni oxide and K-Ca oxide impregnated bituminous and subbituminous chars (TABLE 6). The K-Ca oxide on raw Rosebud char has the lowest activation energy.

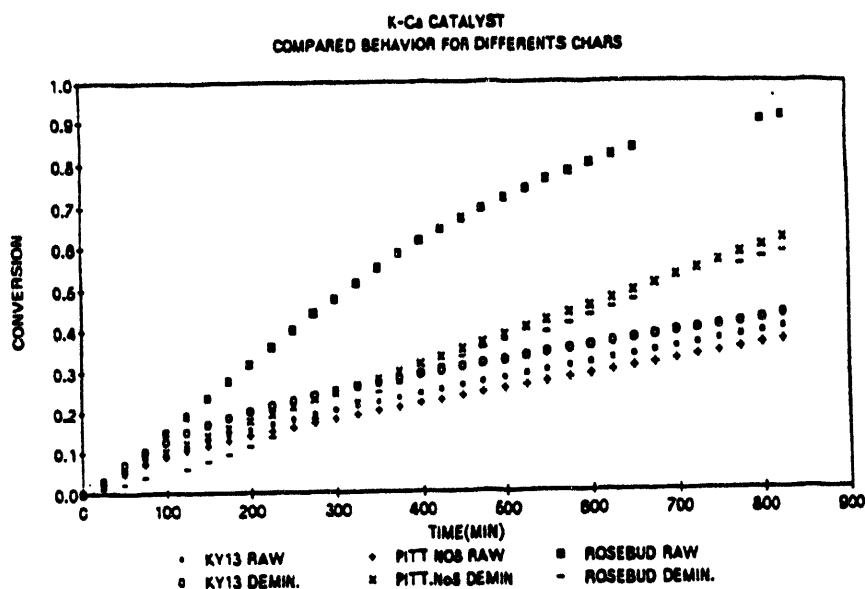


FIG. 24. Comparison of behavior of two bituminous (KY 13, Pitt #8) and one subbituminous (Rosebud) chars before and after demineralization for steam gasification in the presence of K-Ca-O<sub>x</sub> catalyst.

TABLE 6. Arrhenius Analysis for Different Catalysts and Chars

Catalyst + Char	Activation Energy (kJ/mol, kcal/mol)	Frequency Factor	Min. Squares Reg. Factor (No. Values)
K-Ca + Pitt No. 8 Franklyn Char	268.7 64.4	$2.11 \times 10^{10}$	0.996 (5)
K-Ca + Pitt No. 8 Franklyn Demineralized	263.2 63.1	$2.22 \times 10^{10}$	0.986 (5)
K-Ni + Pitt No. 8 Franklyn Char	225.6 54.1	$4.90 \times 10^9$	0.9098 (4)
K-Ca + Rosebud Char Demineralized	240.9 57.8	$2.22 \times 10^9$	0.977 (6)
K-Ca + Rosebud Char	202.2 48.6	$3.61 \times 10^9$	---

### 3) Ternary Catalysts.

Steam gasification of an Illinois #6 char was investigated with catalysts comprising three metal oxide components, usually potassium and calcium oxides with an additional ingredient of either nickel, cobalt, molybdenum, tungsten, vanadium or iron. TABLE 7 shows the selectivities of these catalysts. The catalysts were prepared by impregnating an Illinois #6 char with enough sodium hydroxide to amount to 0.2% sodium oxide on the basis of carbon in the char. The thus impregnated char was dried and calcined at 500 °C and then impregnated with equimolar solution of 3 metal carbonates, the total of metal oxides amounting to 1% of the carbon content of the char.

TABLE 7 shows the selectivities of catalysts comprising potassium and calcium oxides together with either nickel, cobalt, molybdenum, tungsten, vanadium or iron oxides, and also shows the selectivity of a sodium hydroxide-free catalyst and a catalyst comprising just 0.2% sodium hydroxide. It is obvious that the tri-component catalysts are better than a single-component catalyst and that of those tested, catalysts comprising nickel and cobalt are appreciably superior to all the others tested, except for the K-Ca-Fe<sup>+3</sup> material. It must be assumed that the K-Ca-Co oxide combination is preferable because it will be less sensitive to sulfur poisoning than either the nickel or iron containing catalysts.

TABLE 7. Selectivities of Catalysts in the Steam Gasification of Illinois #6 Char (640 °C)

Catalysts	Selectivity CO %	Selectivity Methane %	Selectivity CO <sub>2</sub> %	Cumulative* Cov. %
NaOH-free	39.4	6.0	54.6	3.12
NaOH (0.2%)	36.2	6.8	57.0	7.65
K-Ca/NaOH (0.2%)	12.7	3.3	86.0	19.20
K-Ca-Ni/NaOH (0%)	22.2	2.6	75.3	8.56
K-Ca-Ni/NaOH (0.2%)	23.2	3.1	73.6	21.50
K-Ca-Co/NaOH (0.2%)	16.1	1.9	82.0	27.30
K-Ca-Mo/NaOH (0.2%)	22.3	2.8	74.9	16.01
K-Ca-W/NaOH (0.2%)	23.3	4.4	72.3	14.50
K-Ca-V/NaOH (0.2%)	28.2	3.4	68.4	12.10
K-Ca-Fe <sup>+2</sup> /NaOH (0.2%)	19.4	1.9	78.7	17.20
K-Ca-Fe <sup>+3</sup> /NaOH (0.2%)	16.0	2.0	82.1	21.35

\*Cumulative conversion of carbon after 300 minutes.

#### 4) Operation at Elevated Pressure.

The effect of pressure was evaluated for a char both in the absence and presence of catalysts. The char was obtained by heating Illinois #6 coal (Argonne Premium high-volatile bituminous) at 10 °C/min to 500 °C and holding for two hours. The K-Ca catalyst was added to the char by impregnation with a solution containing equimolar amounts of potassium nitrate and calcium nitrate, followed by drying at 200 °C for 10 hours. Catalyst loading was K:Ca:C = 1:1:100, assuming 80 wt % C in the char. FIG. 25 is a graph of the carbon conversion *vs.* time, showing the effects of catalysts and pressure on the gasification of char. It is apparent that the catalyzed char reacts over twice as fast as the uncatalyzed char. The increase in conversion stems from an increase in hydrogen and CO<sub>2</sub> production. Pressure is seen to have a small enhancing effect on the uncatalyzed char and no apparent effect on conversion of the major products of the catalyzed char. It does seem to affect the relative amounts of the minor products CO and CH<sub>4</sub>, which are produced in quantities that are on order of magnitude lower than H<sub>2</sub> and CO<sub>2</sub>. FIG. 26 shows the production rate of CO and methane as a function of time for the catalyzed char. The production of CO is depressed at 100 psig while methane production is enhanced and by roughly half the amount of the depres-



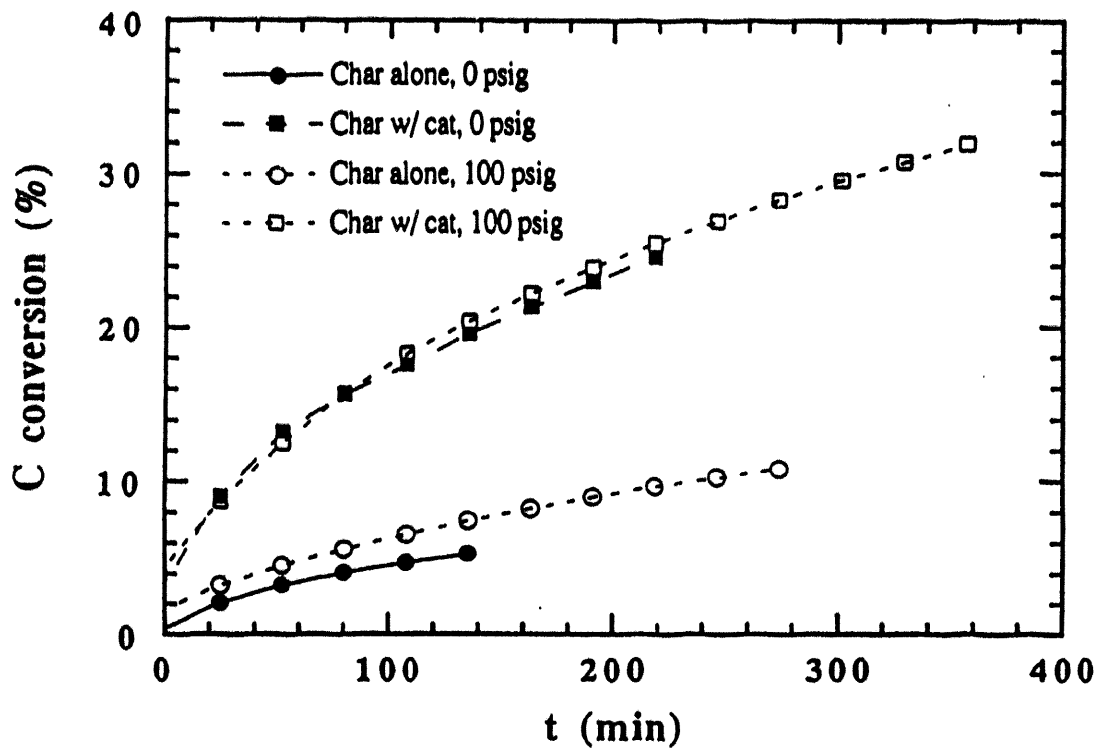


FIG. 25. Effect of pressure on gasification of Illinois #6 char in the presence and absence of catalyst.

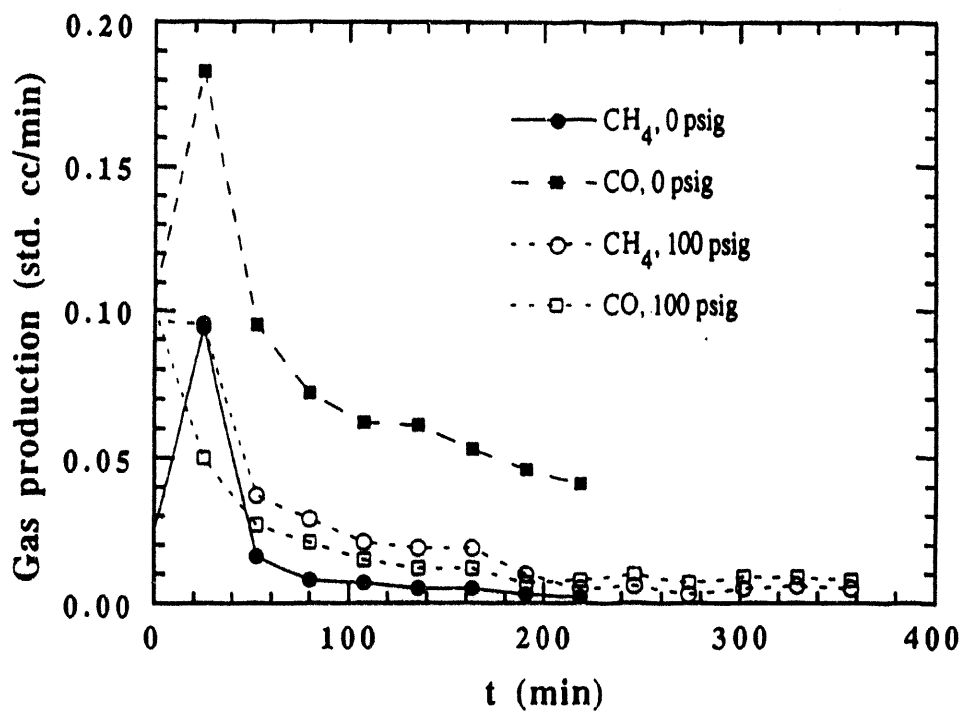
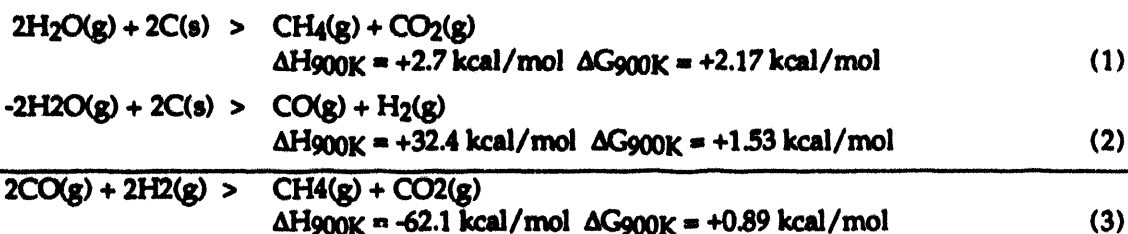


FIG. 26. Methane and CO production during gasification at various pressures.

sion in CO. This could occur in accordance with reactions (1) (2) (3) in which the overall equation (3) has a decrease in gas phase modes which would be more favored at high pressure.



#### 5) Chars Prepared in the Presence of Alkali.

During experimentation with petroleum cokes (see SEC. VI-D), it was first found that coking of petroleum resids in the presence of some alkali greatly enhanced the gasification characteristics of the coke. This work was extended to charring coals in the presence of small amounts of sodium or potassium hydroxide. As in the case of petroleum cokes, the resulting chars showed considerably better gasification characteristics than those prepared in the absence of alkali.

The caustic containing chars were obtained by adding a NaOH solution (10 or 20 wt % NaOH, 8.5% of the coal weight) to the coals prior to charring. Argonne Premium coals (Illinois #6 high-volatile bituminous and Wyoming sub-bituminous) were charred at 500 or 640 °C for two hours. Swelling of the Illinois coal was eliminated by the alkali addition, consistent with published results.

The effects of sodium hydroxide loading and pyrolysis at two temperatures on the rate of steam gasification of Illinois #6 bituminous coal chars are shown in FIG. 27. Differences in the activity are evident in the plots of carbon conversion as a function of time. The Illinois #6 high-volatile bituminous coal was charred without any NaOH (closed symbols) and with the addition of solutions (8.5 wt % of loading) containing 10% NaOH (closed symbols) or 20% NaOH (open symbols). Charring temperatures were 500 °C (circles) and 640 °C (squares). Gasification was at 640 °C. Increasing alkali loadings increases the initial gasification rate for the chars produced at 500 °C. Increasing pyrolysis temperature without any caustic during charring decreases the steam gasification rate at low conversions, but not at higher conversions. When using NaOH, charring at 640 °C gave chars that were much less reactive

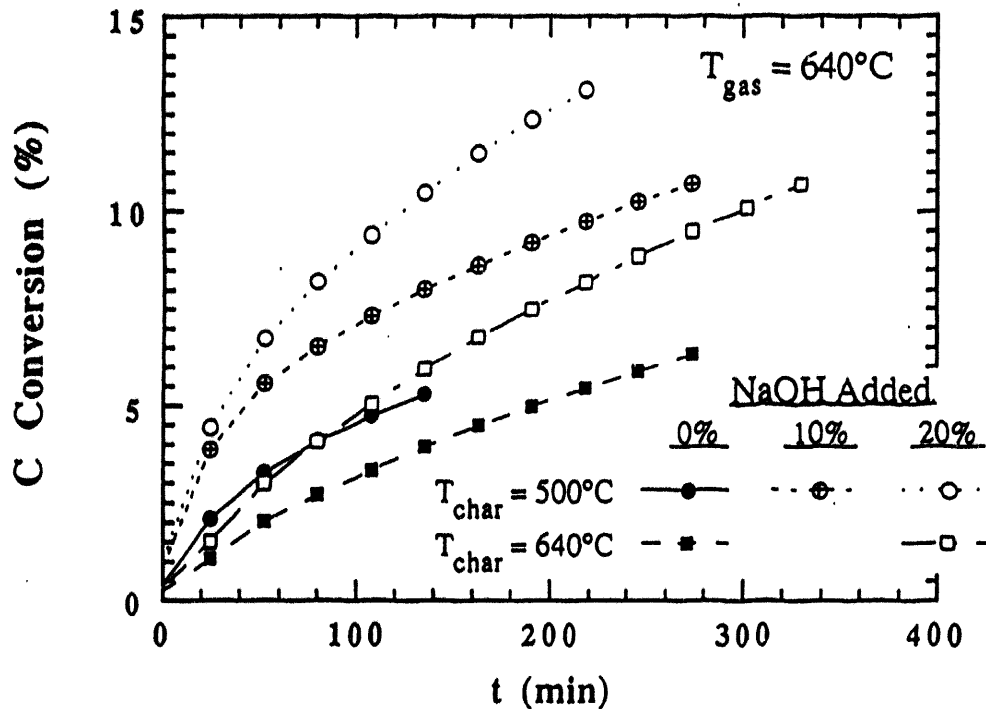


FIG. 27. Comparison of steam gasification reactivity for chars obtained at different charring temperatures and at different NaOH loadings.

through 10% conversion than the low-temperature chars. TABLE 8 shows the sodium content of the chars and of the residues remaining after gasification. The values were normalized to the content of calcium as it should not be consumed during charring or gasification. The sodium content is observed to decline during gasification for all samples, particularly for the chars made with NaOH. Gasification causes a larger reduction in sodium from the 640 °C char than the 500 °C char.

TABLE 8. Na/Ca Weight Ratios of Illinois #6 Coal, Chars and Gasification Residues

Sample	Na/Ca wt ratio	
	In sample before gasification	In residue after gasification at 0 psig/100 psig
raw coal	0.088	
500 °C char	0.051	0.024/0.015
640 °C char	0.022	0.018
500 °C char with 20% NaOH	1.168	0.963/0.406
640 °C char with 20% NaOH	1.163	0.768

FIG. 28 shows how charring with NaOH and addition of the K-Ca oxide catalyst affects steam gasification of Illinois #6 chars. The carbon conversions are compared for chars that were obtained without (circles) and with (squares) 8.5 wt % loading of 20% NaOH for uncatalyzed (closed symbols) and catalyzed (1% K-Ca oxide catalyst; open symbols) steam gasification. For the NaOH-free char, gasification with the catalyst is much faster and more persistent. For the NaOH containing char, the enhancement of gasification due to the addition of the catalyst is even greater.

To reveal possible roles of residual sodium hydroxide in chars prepared in the presence of sodium hydroxide, gasification experiments were conducted with chars after being washed in hot water. The latter treatment was to remove potential residual sodium hydroxide in chars. To remove residual sodium hydroxide, the chars were washed three times in hot water (under refluxing and constant stirring, 1 gm of char in 200 gm of distilled water). The washed chars were dried at 110 °C before being used for gasification.

FIG. 29 presents data of carbon conversion of Illinois #6 coal chars prepared with different NaOH loadings. Washing of the chars after preparation resulted in lower gasification rates than

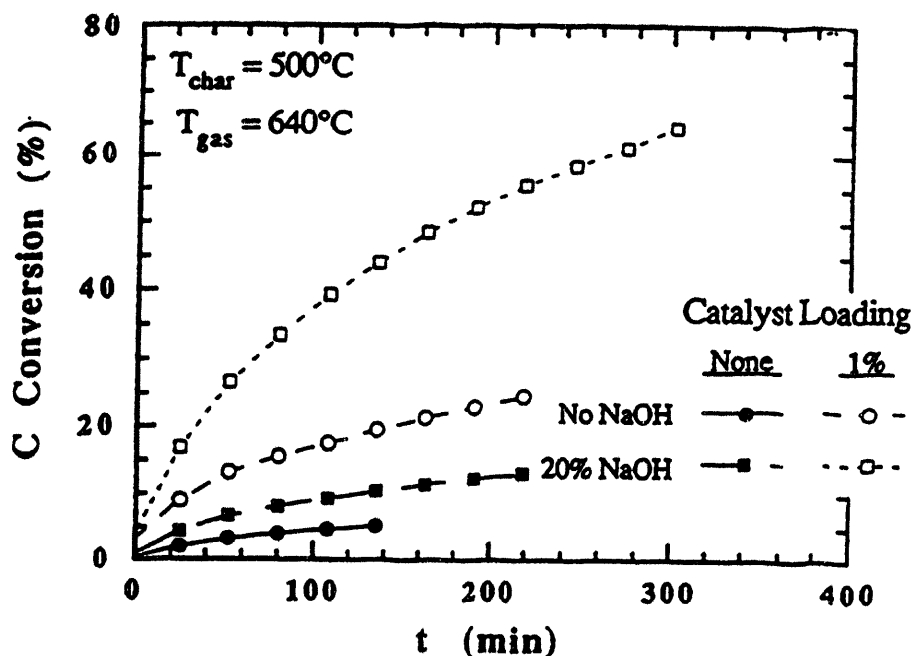


FIG. 28. Comparison of catalyzed and uncatalyzed steam gasification reactivity of chars with different NaOH loadings. K-Ca catalyst loading is 1%.

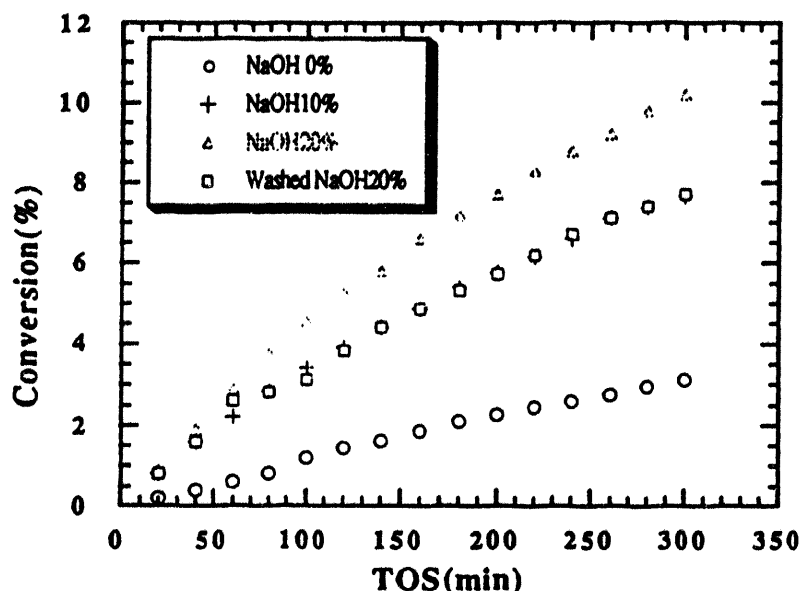


FIG. 29. Effect of residual NaOH on Illinois #6 char conversion.

using the unwashed char. However, the gasification rate of the washed char was still appreciably higher than that of the char prepared in the absence of caustic.

Results obtained using different catalysts are given in TABLE 9. The presence of catalysts significantly enhanced the gasification of char. Catalysts containing transition metals are more effective than binary K-Ca oxide catalysts. It seems that cobalt is more active than nickel.

TABLE 9. Effect of Catalyst on Illinois Char (20% NaOH)

Catalyst	Carbon Conversion % <sup>a</sup>
—	10.2
K-Ca	19.2
K-Ca-Ni	21.5
K-Ca-Co	27.5

<sup>a</sup>conversion at time on stream of 300 min.

6) *Use of Alkali by Steam Entrainment.*

It has been shown that effects similar to those obtained by charring coals in the presence of alkali can be obtained by introducing alkali into the reactor together with the steam. This was achieved by gasifying a 1% sodium hydroxide solution and in-

roducing the steam into the reactor. Since it is not possible to gasify NaOH at these temperatures, effects observed are obviously due to entrainment of caustic particles in the steam. FIG. 30 compares the effect of using gasification of a 1% NaOH solution during gasification with the gasification of an untreated char, and FIG. 31 presents similar data for chars impregnated with a K-Ca oxide catalyst.

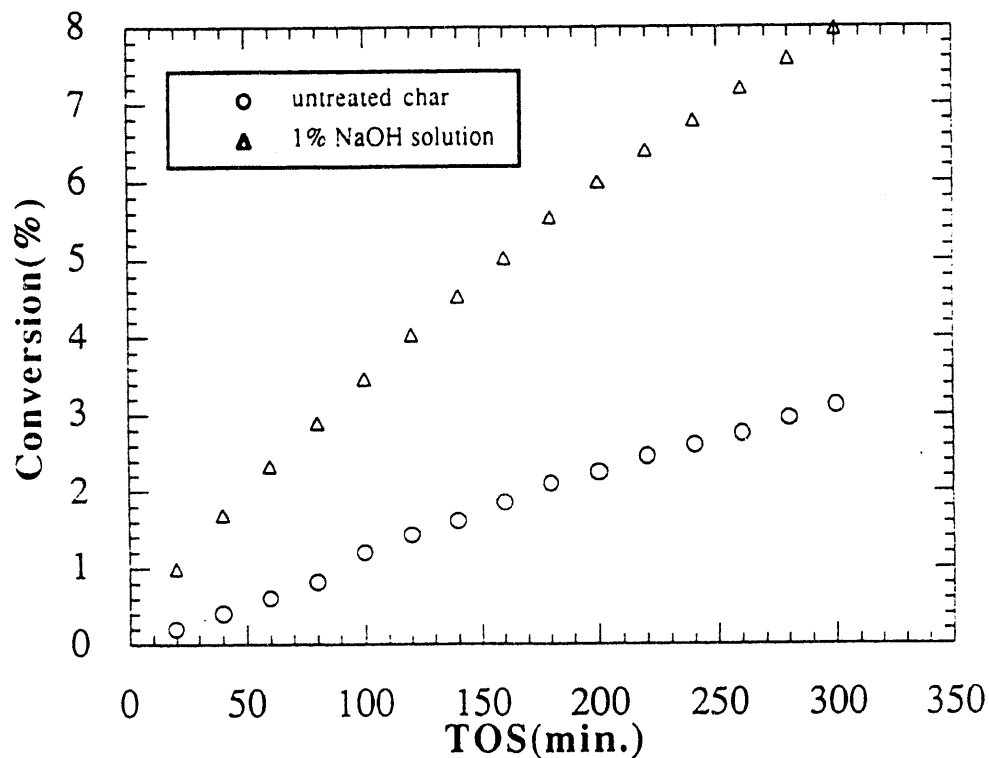


FIG. 30. Comparison data of additive effect (1 wt % NaOH solution, used to make steam)

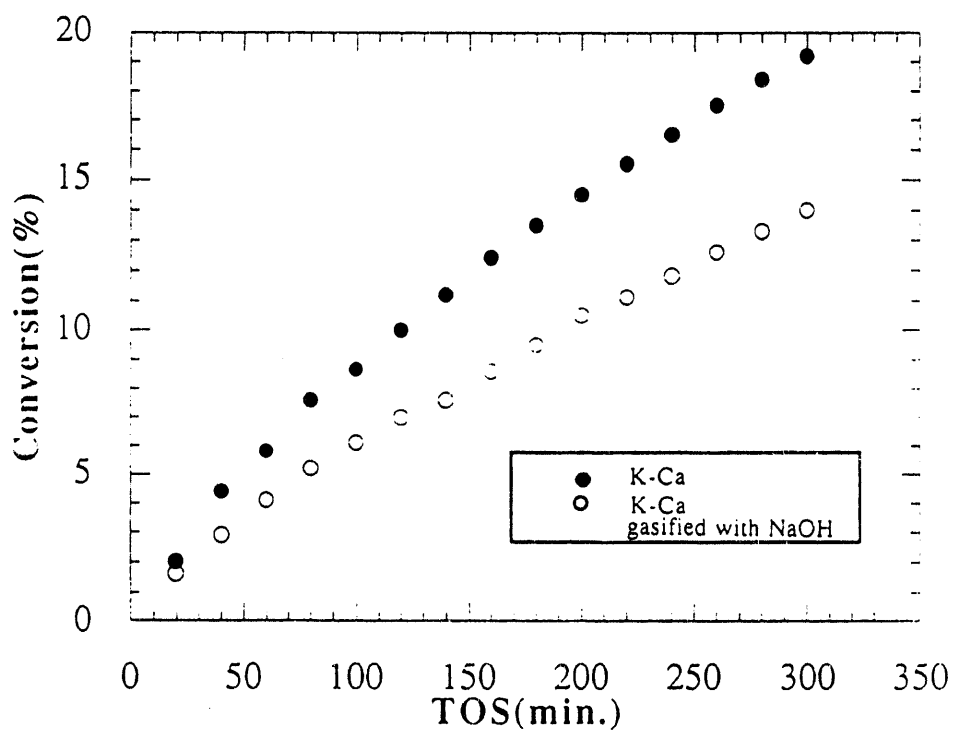


FIG. 31. Comparison data of additive effect (1 wt % NaOH solution, used to make steam)

## C Steam Gasification of Coals

### 1) Kinetics.

Samples of three coals were obtained from IGT. These are the parent coals of the chars which have been used in earlier work. They comprise a subbituminous (Rosebud) and two bituminous coals (Ohio Pitt #8 and Kentucky #13). An analysis of these coals is given in TABLE 10.

The three coals were subjected to steam gasification at 640°C both in the absence of and in the presence of K-Ca-O catalyst. When the catalyst was used, it was impregnated on the coal by an aqueous nitrate solution containing equimolecular amounts of K and Ca. The procedure used and the nitrate decomposition treatment were the same as previously described for chars and graphite.

In the absence of catalysts no gasification occurred except for an evolution of light hydrocarbons (devolatilization) during the heat-up period. This was most pronounced for the subbituminous Rosebud coal.

In the presence of catalysts, gasification of all three coals was quite rapid and much faster than that of the corresponding chars, which in turn gasified better than graphite. Complete (100%) gasification of all coals was achieved at 640°C. The subbituminous Rosebud coal gasified better than the bituminous coals.

FIG. 32 plots the catalytic gasification of Rosebud coal at two temperatures, 580 and 640°C. The gasification occurring at the lower temperature is essentially only a devolatilization. However, while in the absence of catalysts the products of this devolatilization were mostly light paraffins and aromatics, in the presence of catalyst, a majority of the products consisted of H<sub>2</sub> and CO<sub>2</sub>, indicating that the catalyst has steam reforming activity at this low temperature.

For all the coals, there is some devolatilization while heating up and before actual carbon gasification occurs. This explains why carbon gasification starts only after 10-25% conversion. FIG. 33 presents a comparison of the three coals investigated. The two bituminous coals have the same steady gasification rate except for the devolatilization part. The Ohio Pitt #8 has



TABLE 10. Proximate, Ultimate and Inorganic Chemical Analyses of Coals Used in Gasification Tests (data supplied by I.G.T.)

Seam	OH Pitt No. 8					
Mine	Franklin 125		KY #13		Rosebud	
<i>Proximate Analysis, wt %</i>						
Moisture	2.5		9.8		23.1	
Volatile Matter	38.6		32.2		28.5	
Ash	7.5		7.3		11.3	
Fixed Carbon	51.4		50.7		37.1	
TOTAL	100.0		100.0		100.0	
<i>Ultimate Analysis, wt % (dry basis)</i>						
Ash	7.68		8.08		14.66	
Carbon	74.47		73.74		62.76	
Hydrogen	5.24		4.82		4.40	
Sulfur	3.21		1.40		1.29	
Nitrogen	1.50		1.8		0.99	
Oxygen (by difference)	7.90		10.11		15.88	
TOTAL	100.00		100.00		100.00	
<i>Ash Composition, wt %</i>						
SiO <sub>2</sub>	41.6		58.5		48.8	
Al <sub>2</sub> O <sub>3</sub>	20.9		26.9		23.5	
Fe <sub>2</sub> O <sub>3</sub>	31.7		8.1		7.02	
TiO <sub>2</sub>	1.02		0.87		0.12	
P <sub>2</sub> O <sub>5</sub>	0.07		0.16		0.25	
CaO	1.14		0.90		7.16	
MgO	0.36		1.21		2.57	
Na <sub>2</sub> O	0.35		0.24		0.09	
K <sub>2</sub> O	0.98		2.94		0.36	
SO <sub>3</sub>	1.00		0.80		9.91	
TOTAL	99.2		100.6		99.78	
<i>Ash Content (as ashed for analysis of ash, dry basis)</i>						
	7.7		8.2		—	
<i>Basic Ash Constituents, wt %</i>						
	35.2		13.4		19.22	
<i>Dolomite Ratio, wt %</i>						
	4.3		15.8		56.6	
<i>SiO<sub>2</sub>/Al<sub>2</sub>O<sub>3</sub> Ratio</i>						
	2.0		2.2		2.1	
<i>Forms of Sulfur, wt % (dry basis)</i>						
Pyritic	2.37		0.40		0.76	
Sulfate	0.21		0.10		0.015	
Organic	0.97		1.03		0.52	
TOTAL	3.56		1.53		1.28	
<i>Forms of Iron (dry basis)</i>						
	wt %	% of Fe	wt %	% of Fe	wt %	% of Fe
Pyritic	2.07	96	0.35	70	1.32	62 <sup>a</sup>
HCl-soluble	0.08	4	0.15	30	0.12	6
TOTAL	2.15	100	0.50	100	2.13 <sup>a</sup>	100
<i>Acid-insoluble</i>						
	<0.10	—	<0.10	—	0.69	—
<i>Pyritic, % of total Fe**</i>						
	97		54		—	

<sup>a</sup>Based on total iron, including 0.69 wt % HCl-insoluble

<sup>b</sup>Of 1/4-inch-top size coal after storage

more volatiles in the presence of steam and catalyst than Kentucky #13. This is somewhat different than the volatile matter content given in TABLE 6 determined in the absence of steam. The subbituminous Rosebud coal shows a better gasification rate than the bituminous coal.

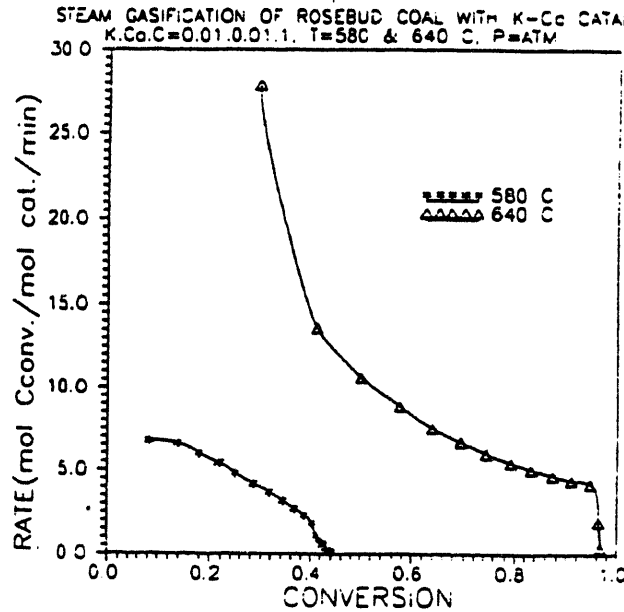


FIG. 32. Catalyzed steam gasification of subbituminous (Rosebud) coal at two temperatures.

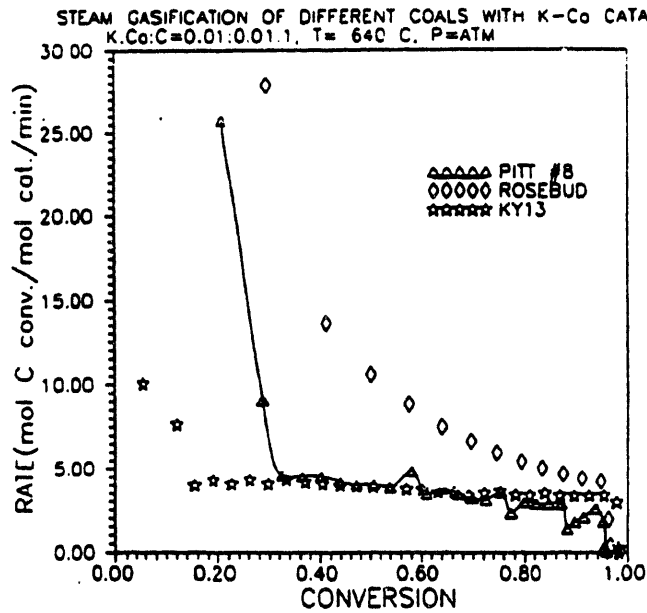


FIG. 33. Comparison of the rate of catalyzed steam gasification of bituminous and subbituminous coals.

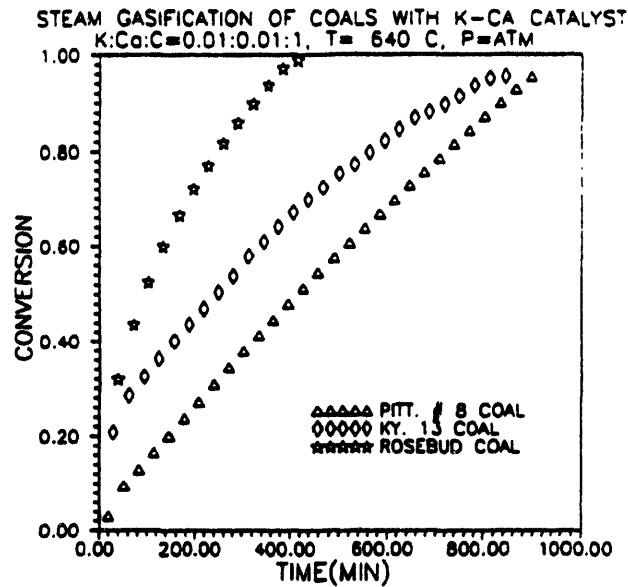


FIG. 34. Comparison of the conversion of bituminous and subbituminous coals during catalyzed steam gasification.

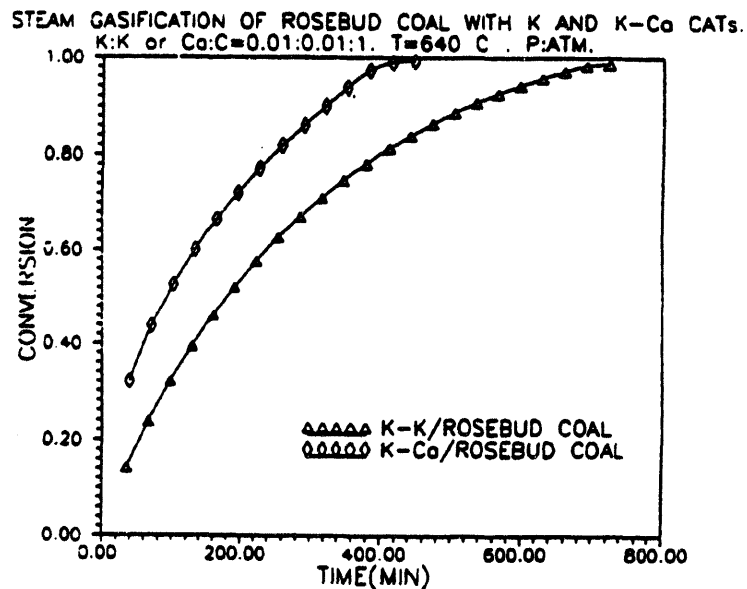


FIG. 35. Comparison of K-Ca-O catalyst with potassium alone for the steam gasification of subbituminous coals.

FIG. 34 presents conversion of the three coals as a function of time. It shows that the Rosebud subbituminous coal is fully gasified in about one-half the time required for the bituminous coals. FIG. 35 demonstrates the advantage of a K-Ca catalyst over K alone for the Rosebud coal. Complete gasification is achieved with K-Ca in about 16% of the time required for K.

A comparison of the Rosebud coal with the Rosebud char (gasification of this was reported in SEC. VI-B.2) is shown in FIGS. 36 and 37. The coal gasifies at a much higher rate than the char. Complete carbon conversion occurs in 450 min for the coal, 900 min for the char (FIG. 36).

The distribution of gases produced from the coals in the presence of K-Ca is illustrated in FIG. 37, plotting conversion

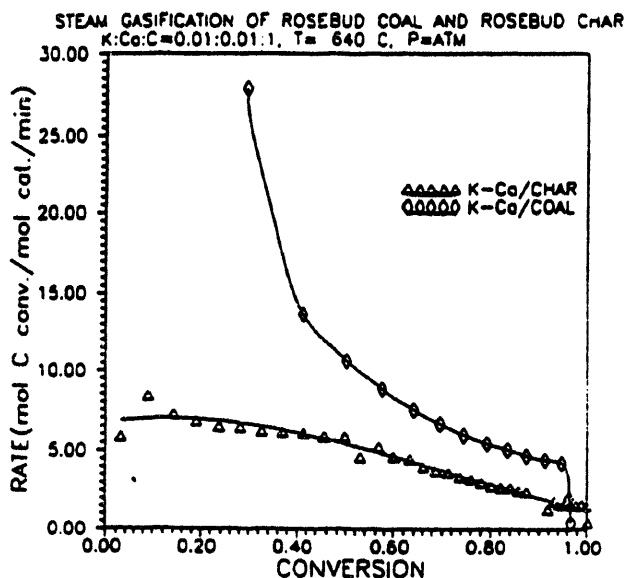


FIG. 36. Comparison of the rates of catalyzed steam gasification of a subbituminous coal and of the char derived from it.

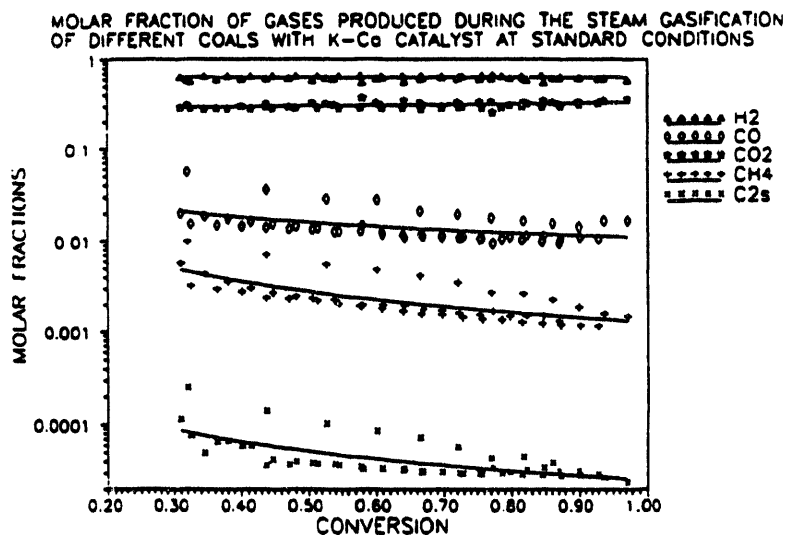


FIG. 37. Gas distribution during catalytic steam gasification of coals, excluding volatilization period.

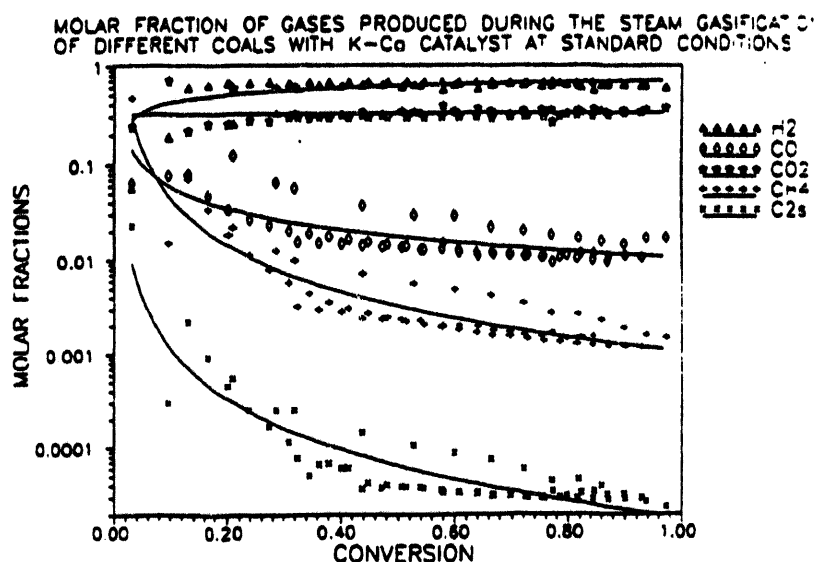


FIG. 38. Gas distribution during catalytic steam gasification of coals, including volatilization period.

*vs.* molar fractions of gases on a logarithmic scale. Hydrogen and carbon dioxide production is steady at a 2:1 ratio over the whole range of conversions while CO, CH<sub>4</sub> and C<sub>2</sub> production gradually decline. CO production amounts to about 2%, CH<sub>4</sub> to 0.5% and C<sub>2</sub> to less than 0.01%. Rosebud coal gives slightly higher yields of CO, CH<sub>4</sub>, and C<sub>2</sub> than the other coals.

While FIG. 37 shows gas distribution after devolatilization, FIG. 38 includes the devolatilization period. During this period (first 30% of conversion) larger amounts of CH<sub>4</sub> and C<sub>2</sub> hydrocarbons (and somewhat higher amounts of CO) are produced. It is remarkable, however, that the major products are again H<sub>2</sub> and CO<sub>2</sub>, indicating that steam reforming of paraffins and aromatics must occur.

## 2) Catalyst Modifications.

In order to test the necessity of using relatively expensive potassium as a catalyst component, gasification of the Ohio Pitt #8 coal was undertaken employing a Na-Ca catalyst. The proportions of Na in the catalyst were the same as in the case of K-Ca. As shown in FIG. 39, the Na-Ca catalyst was at least as active as K-Ca, increasing the likelihood that the catalyst may be used on a throw-away basis.

STEAM GASIFICATION OF PITT #8 WITH Na-Ca CATALYSTS  
 Na:Ca:C=0.01:0.01:1. - STANDARD CONDITIONS

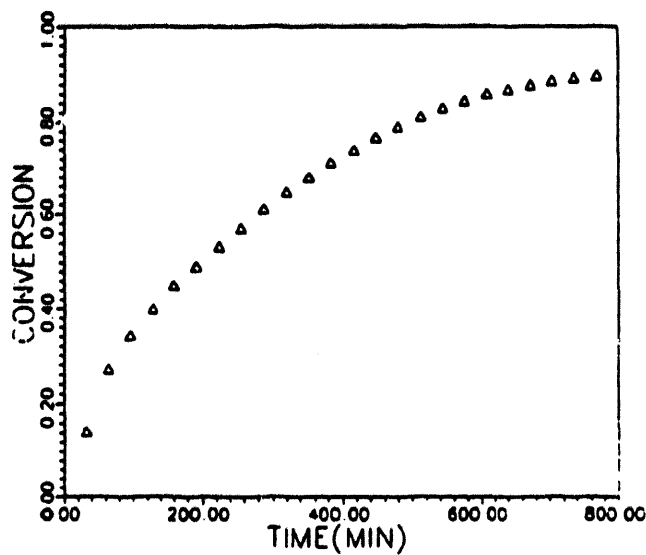


FIG. 39. Conversion of a bituminous coal in the catalytic steam gasification using a sodium-calcium oxide rather than the potassium equivalent.

A catalyst comprising cesium-calcium was also tested. It exhibited almost no gasification activity. The reason for this may lie in the large atomic size of the Cs relative to Ca.

Negative results were obtained when it was attempted to improve the K-Ca-O<sub>x</sub> catalyst by incorporating a third oxide component. A standard K-Ca-O<sub>x</sub>-impregnated Rosebud coal was further impregnated with Ni(NO<sub>3</sub>)<sub>2</sub> solution (Ni = 1/2 of molar K-Ca content) and then dried and decomposed by standard procedure. The thus prepared coal was less active than the K-Ca-O<sub>x</sub>-impregnated coal, perhaps because the Ni blocked access to some of the K-Ca-O<sub>x</sub> sites.

FIG. 40 extends earlier work comparing the relative activity of K-Ni-O<sub>x</sub> and K-Ca-O<sub>x</sub> catalysts from chars to coals. Ohio Franklin Pitt #8 coal was impregnated with K-Ca-O<sub>x</sub> and with K-Ni-O<sub>x</sub>. Just as in the case of chars, K-Ca-O<sub>x</sub> was more active in gasifying the coal than was K-Ni-O<sub>x</sub>. This result further confirms earlier conclusions that K-Ca-O<sub>x</sub> is more active than K-Ni-O<sub>x</sub> for high rank coals.

Impregnation of Franklin Pitt #8 coal with other alkali and/or earth alkali oxides was undertaken. It was previously shown that Na could be substituted for K without adverse effects. Using a cesium-barium nitrate aqueous solution for impregna-

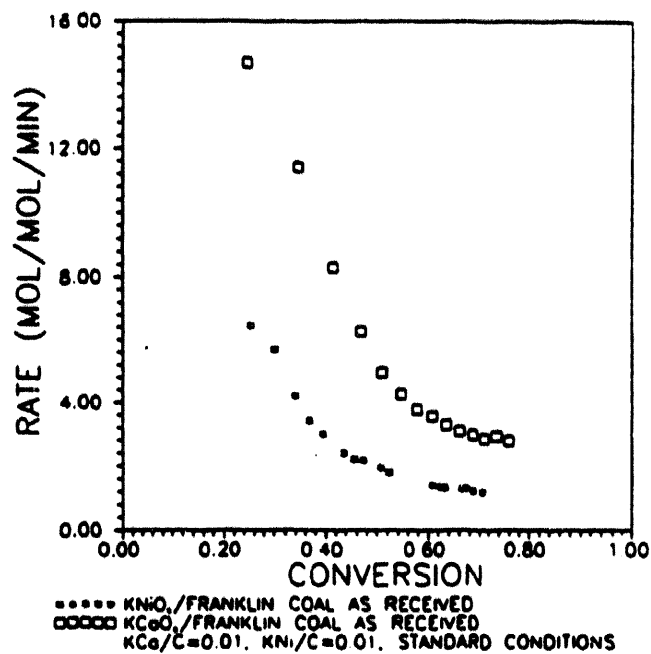
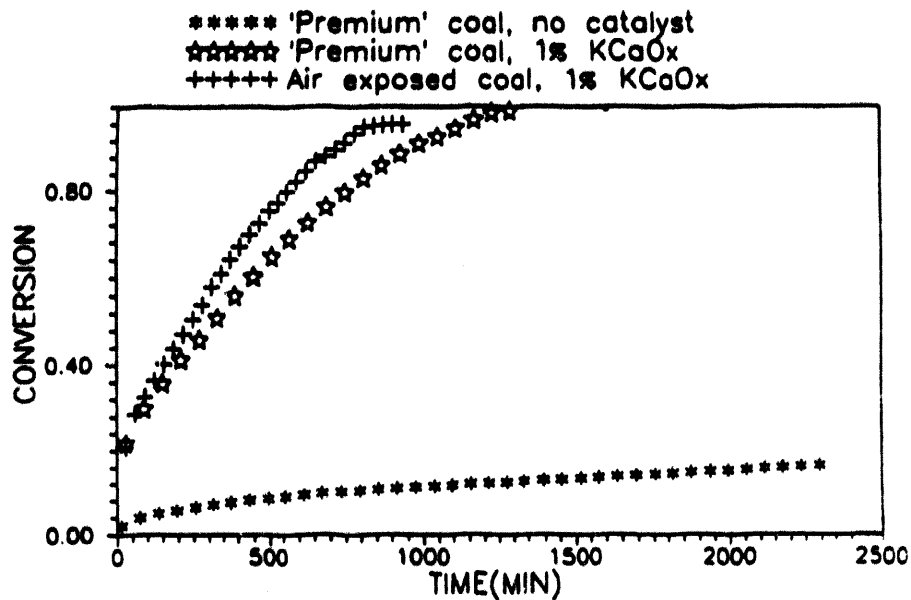


FIG. 40. Comparison of Ni-K-Ox and Ca-K-Ox catalysts for the steam gasification of a bituminous coal.

tion and following the standard drying and decomposition procedure, the Cs-Ba-O<sub>x</sub> catalyst behaves similarly to K-Ca-O<sub>x</sub>.

Coal samples previously used in this work had been obtained from IGT and had been stored there and in our laboratory under conditions which may have led to a surface oxidation of the coal. Samples of "premium" coals were obtained from the coal bank at the Argonne National Laboratory, which were mined, crushed and stored under atmosphere-controlled conditions and which can be assumed not to have been contaminated by atmospheric oxygen. The Pitt #8 Franklin "premium" coal has been gasified under our standard conditions and compared with the gasification of the same coal which had been stored without precautions. FIG. 41 presents a time *vs.* conversion plot for the "premium" coal in the absence of catalyst, and for both coals in the presence of K-Ca-O<sub>x</sub> catalyst. The "premium" coal in the absence of catalyst showed only very minor gasification characteristics at standard conditions. The two coal samples impregnated with 1% K-Ca-O<sub>x</sub> behaved very similarly with a slight advantage for the air-exposed coal. It is concluded that exposure to air is not detrimental to the gasification of coals and that no special precautions have to be taken in preparing the coals for gasification.



STEAM GASIFICATION OF PITT. #8 FRANKLIN COAL AT 640 C.  
 0.5 g. of sample, water flow: 4 g./h.  
 'Premium' coal is compared to a long time air exposed  
 coal in presence or absence of KCaOx catalyst.

FIG. 41. Comparison of steam gasification of a fresh bituminous coal with a surface oxidized coal.



## D) Steam Gasification of Petroleum Cokes

In an attempt to determine the effect of metals in the substrate on catalytic gasification, a series of petroleum cokes with different compositions and metal contents were gasified. The approximate composition of the cokes is shown in TABLE 11. It is apparent that there are wide variations of sulfur content (0.6-8%), of metal content (116-4011 ppm), and metal distribution between Ni, V, and Fe. Coke samples were supplied by Mobil Research and Development Corporation.

The cokes were impregnated with 1 mol % of a catalyst comprised of equimolar calcium and potassium oxides for a Ca + K/C atomic ratio of 0.04. Gasification was at 600° C using 8 cc water per gram of carbon per hour at atmospheric pressure. Results of the gasification of several of the cokes are shown in FIG. 42.

It is apparent from FIG. 42 that all but one of the cokes tested were easily gasified in the presence of catalyst and that their gasification rate was somewhere between those of subbituminous and bituminous coals. The relatively poor performance of Coke #1 is unexplained and cannot be attributed to metals, sulfur or high carbon content, since these (as shown in TABLE 11) are not essentially different from some of the other cokes. This particular coke behaves more like graphite. It is also the most aromatic coke.

During the work on steam gasification of cokes impregnated with catalysts, it was discovered that considerable improvements in gasification rates could be obtained by coking the petroleum resid in the presence of small amounts of caustic. The gasification rate for a coke prepared by coking in the presence of caustic is better than that for a coke containing a potassium-calcium catalyst impregnated directly on the coke prepared in

TABLE 11. Analytical Data for Petroleum Coke Samples

Number	C (%)	H (%)	O (%)	S (%)	Ni (ppm)	V (ppm)	Fe (ppm)	Total Metals (ppm)
1	87.6	3.55	2.39	2.55	707	1090	832	2629
2	86.1	3.61	1.48	6.12	422	1919	1166	3507
3	92.8	3.90	1.41	0.55	147	20	3844	4011
4	88.6	3.76	0.97	5.13	223	657	209	1089
5	87.7	3.18	1.07	5.62	334	809	536	1679
6	90.9	4.0	0.42	4.45	12	5	99	116
7	86.6	3.35	0.93	7.96	175	509	178	862

COKES WITH CATALYST(K<sub>2</sub>CO<sub>3</sub>). STANDARD CONDITIONS  
CONVERSION VS TIME

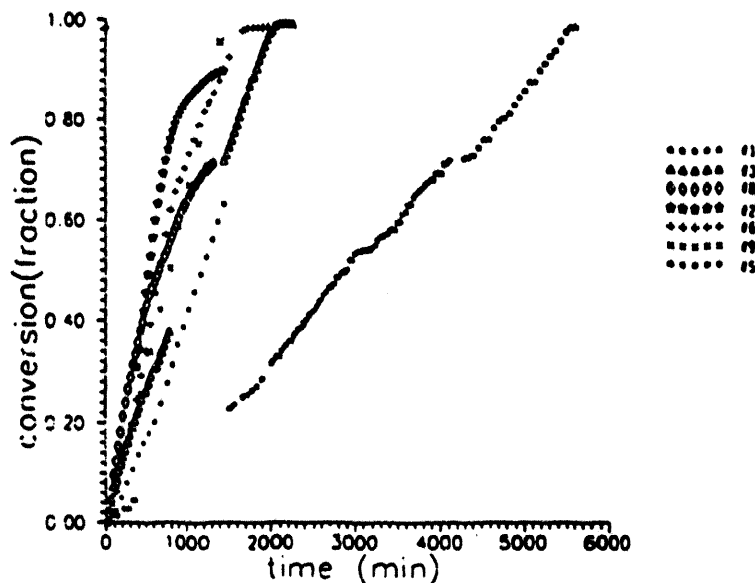


FIG. 42. Catalytic steam gasification of petroleum cokes. Dissociate water at reaction temperature.

the absence of caustic. When a coke prepared in the presence of caustic is then impregnated with the potassium-calcium oxide catalyst, a further major improvement in gasification rate is obtained. It has further been shown that the alkali used for coking may be derived from byproducts of petroleum refining such as sulfur containing caustic streams. The sulfur which is thus incorporated into the coke will then be gasified as H<sub>2</sub>S during gasification and the whole process can act as an environmentally desirable operation disposing of sulfur-containing byproducts while also disposing of petroleum coke. This is shown in FIG. 43. FIG. 44 compares gasification of two petroleum cokes coked in the presence of NaOH with similarly prepared Illinois #6 and Wyoming chars, indicating the generic nature of the treatment. FIG. 45 presents the same information for the same materials in the absence of alkali treatment during coking or charring.

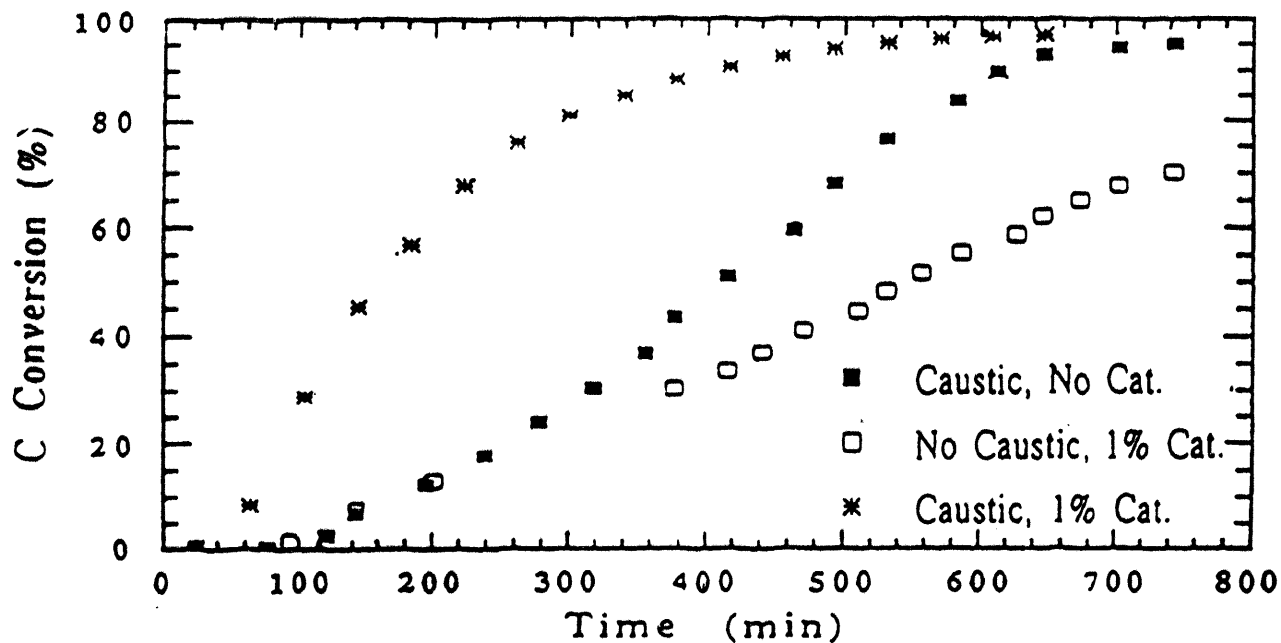


FIG. 43. Conversion of C during steam gasification at 640 °C of Mexican coke obtained with refinery-derived caustic waste (closed squares), with 1% loading of K-Ca catalyst (open squares), and with both caustic and catalyst (asterisks).

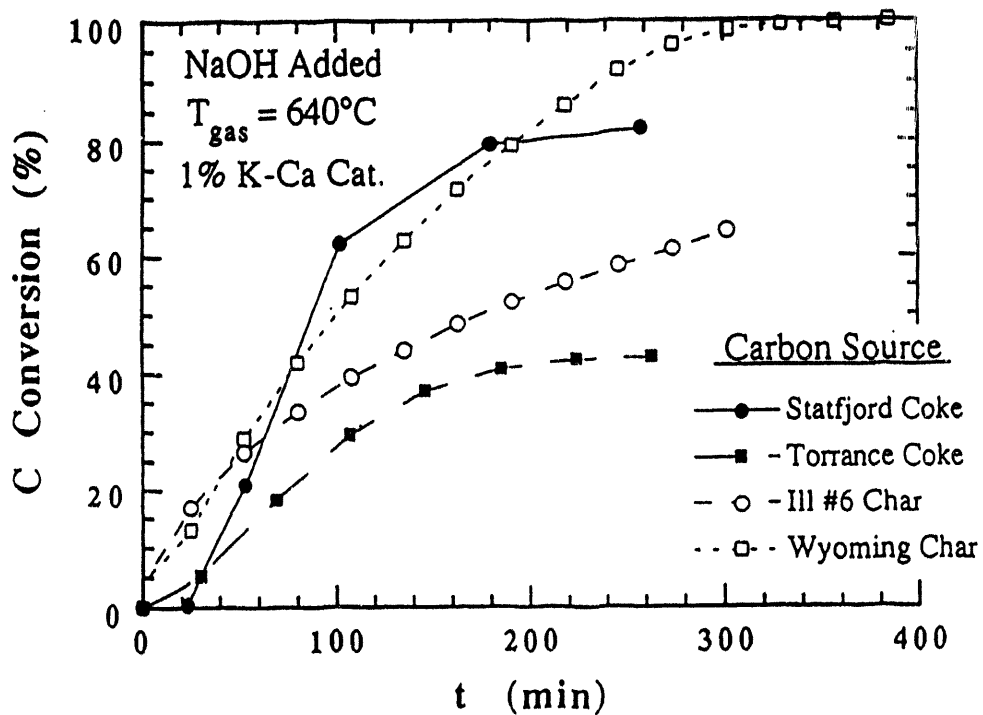


FIG. 44. Steam gasification of petroleum cokes and of coal chars treated with alkali during coking, resp. charring.

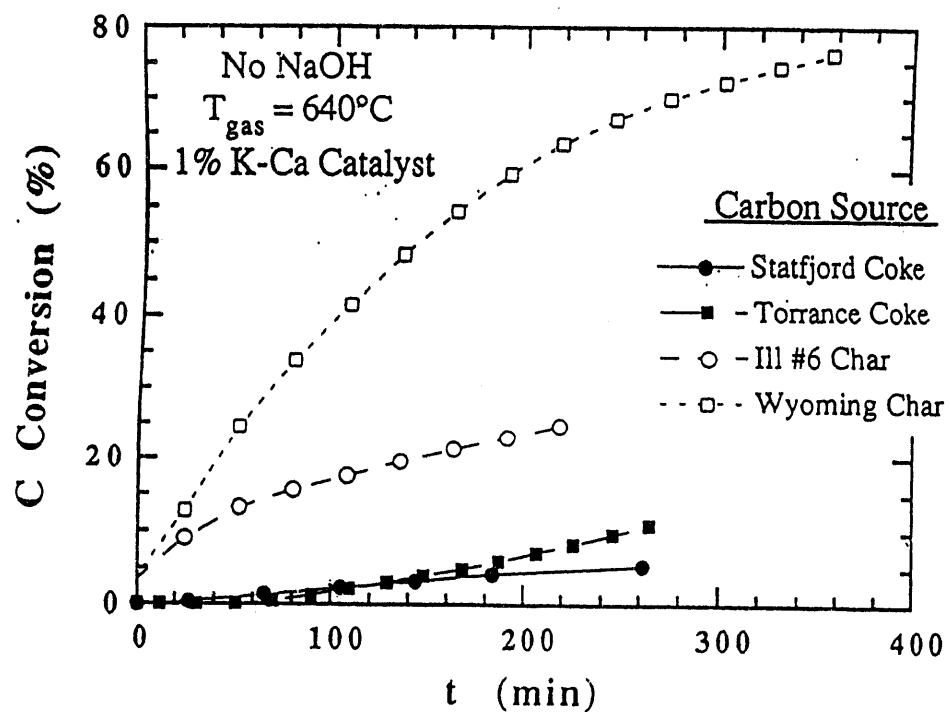


FIG. 45. Steam gasification of petroleum cokes and of coal chars *not* treated with alkali during coking, resp. charring.

## VII. CONCLUSIONS

- Good steam gasification catalysts must:
  - wet the carbonaceous material
  - attack by edge recession
  - dissociate water at reaction temperature.
- The catalytic gasification mechanism involves water dissociation forming  $H_2$  and carbon surface oxygenates (lactones, quinones) and C-CO bond breakage, forming  $CO_2$ . The carbon-carbon bond breakage is the rate-limiting step.
- The mechanism of catalytic gasification of graphite, chars and coals is the same as evidenced by their same activation energy.
- Gasification products are primarily hydrogen and  $CO_2$ .
- K- $CaO_x$  (or  $NaO_x$ - $CaO_x$ ) catalysts equal  $KO_x$ - $NiO_x$  catalysts.
- K- $CaO_x$  catalysts are not poisoned by S, while K- $NiO_x$  is poisoned by organic sulfur.
- K- $CaO_x$  catalysts have good gasification rates at 525-640 °C, giving  $H_2$  and  $CO_2$  from lignite > subbituminous > bituminous chars or coals.
- Some ternary catalysts (e.g., K-Ca-Co oxide) are superior to binary catalysts.
- Coals gasify at better rates than their chars, which gasify better than graphite.
- Petroleum cokes can be catalytically gasified at rates very similar to those of coals.
- Treatment of chars or cokes with small amounts of alkali during preparation enhances their gasification rates. Gasification of thus treated chars and cokes with catalysts results in additional gasification rate improvement.

## VIII. REFERENCES

1. WEN, W.-Y. (1980) *Catal. Rev. Sci.-Eng.* **22** (1), 1.
2. WOOD, B.J. and SANCIER, K.M. (1984) *Catal. Rev. Sci.-Eng.* **26** (2), 233.
3. MIMS, C.A. and PABST, J.K. (1983) *Fuel* **62**, 176.
4. BLAKELY, A.W., KOZAK, E.I., SEXTON, B.A. and SOMORJAI, G.A. (1976) *J. Vac. Sci. Technol.* **13**, 1091.
5. BAKER, R.T.K. and HARRIS, P.S. (1972) *J. Sci. Instrum.* **5**, 793.
6. CABRERA, A.L., HEINEMANN, H. and SOMORJAI, G.A. (1982) *J. Catal.* **75**, 7.
7. COATES, D.J., EVANS, J.W., CABRERA, A.L., SOMORJAI, G.A. and HEINEMANN, H. (1983) *J. Catal.* **80**, 215.
8. DELANEY, F., TYSOE, W.T., HEINEMANN, H. and SOMORJAI, G.A. (1984) *Carbon* **22** (4/5), 401.
9. DELANEY, F., TYSOE, W.T., HEINEMANN, H. and SOMORJAI, G.A. (1984) *Appl. Catal.* **10**, 111.
10. MCKEE, D.W. (1974) *Carbon* **12**, 453.
11. WALKER, P.L., JR. et al. (1983) *Fuel* **62**, 140.
12. YAMADA, T. et al. (1983) *Fuel* **62**, 246.
13. BAKER, M.G. and DAWSON, A.P. (1976) *J. Less Com. Met.* **45**, 323.
14. EROSKISS, K. et al. (1976) *Period Polytech. Chem. Eng.* **20**, 13.
15. ADLER, J. and HÜTTINGER, K.J. (1984) *Fuel* **63**, 1939.
16. ROSTRUP-NIELSEN, J.R. (1975) "Stream Reforming Catalysts," p. 150. Teknisk Forlag A/S, Copenhagen.
17. WIGMANS, T. and MOULIJN, J.A. (1981) *Stud. Surf. Sci. Catal.* **7**, 501.
18. WIGMANS, T. et al. (1983) *Surf. Sci.* **135**, 532.
19. HEINEMANN, H., SOMORJAI, G.A., PEREIRA, P. and CARRAZZA, J. (1989) *Preprints Fuel Div., A.C.S.* **34** (1), 121.
20. MARCHON, B., CARRAZZA, J., HEINEMANN, H. and SOMORJAI, G.A. (1988) *Carbon* **26**, 507.
21. CARRAZZA, J., TYSOE, W.T., HEINEMANN, H. and SOMORJAI, G.A. (1985) *J. Catal.* **96**, 234.
22. BAKER, M.G. and DAWSON, A.P. (1976) *J. Less Com. Met.* **45**, 323.
23. SUZUKI, T., MISHIMA, M. and WATANABE, Y. (1984) *Fuel* **63**, 1393.
24. HOLSTEIN, W.L. (1983) *Fuel* **62**, 259.
25. PEREIRA, P., CSENCISITS, R., SOMORJAI, G.A. and HEINEMANN, H. (1990) *J. Catal.* **123**, 463.
26. PERIERER, A. and GUYAN, E. (1978) *Carbon* **16**, 127.
27. THIEL, P.A., HABEK, J., DEPAOLA, R.A. and HOFFMAN, F.M. (1984) *Chem. Phys. Lett.* **25**, 108.
28. BONZEL, P.H., PIROG, G. and WINKLER, A. (1981) *Surf. Sci.* **175**, 287.

## IX. APPENDIX

Publications of work performed under this contract:

- CABRERA, A.L., HEINEMANN, H. and SOMORJAI, G.A. (1982) "Methane production from the catalyzed reaction of graphite and water vapor at low temperatures (500-600K)," *J. Catal.* **75**, 7-22.
- CABRERA, A.L., HEINEMANN, H. and SOMORJAI, G.A. (1982) "Catalyzed depolymerization of graphite observed by photoelectron spectroscopy," *Scientia* **47** (158/159).
- COATES, D.J., EVANS, J.W., CABRERA, A.L., SOMORJAI, G. A. and HEINEMANN, H. (1983) "An electron microscopy study of the low temperature catalyzed steam gasification of graphite," *J. Catal.* **80**, 215-220.
- CASANOVA, R., CABRERA, A.L., HEINEMANN, H. and SOMORJAI, G. A. (1983) "Calcium oxide and potassium hydroxide catalyzed low temperature methane production from graphite and water: Comparison of catalytic mechanisms," *Fuel* **62**, 1138-1144.
- COATES, D.J., EVANS, J.W., HEINEMANN, H. (1983) "In-situ observations of the gasification of carbon catalyzed by calcium oxide," *Appl. Catal.* **7**, 233-241.
- DELANNAY, F., TYSOE, W.T., HEINEMANN, H. and SOMORJAI, G.A. (1984) "Distribution of reaction products in the KOH initiated low temperature steam gasification of graphite," *Appl. Catal.* **10**, 111-123.
- DELANNAY, F., TYSOE, W.T., HEINEMANN, H. and SOMORJAI, G.A. (1984) "The Role of KOH in the Steam Gasification of Graphite: Identification of the Reaction Steps," *Carbon* **22** (4/5), 401-407.
- CARRAZZA, J., TYSOE, W.T., HEINEMANN, H. and SOMORJAI, G.A. (1985) "Gasification of graphite with steam below 900K catalysed by a mixture of KOH and transition metal oxide," *J. Catal.* **96**, 234-241. LBL-18872.
- HEINEMANN, H. and SOMORJAI, G.A. (1986) "Mechanism of the catalytic gasification and reactivity of graphite," in *Chemical Reactions in Organic and Inorganic Constrained Systems*, pp. 401-410.
- CARRAZZA, J., SOMORJAI, G.A. and HEINEMANN, H. (1986) "Steam gasification of carbonaceous solids catalyzed by a mixture of potassium and

nickel oxides below 1000K", *American Chemical Society, Preprints Petroleum Division* 31 (3), 158-165.

CARRAZZA, J., CHLUDINSKY, J.J., JR., HEINEMANN, H., SOMORJAI, G.A. and BAKER, R.T.K. (1988) "Controlled atmosphere electron microscopy study of the gasification of graphite by water, hydrogen and oxygen catalyzed by a nickel/potassium mixture," *J. Catal.* 110, 76-81.

MARCHON, B., CARRAZZA, J., HEINEMANN, H. and SOMORJAI, G.A. (1988) "TPD and XPS studies of O<sub>2</sub>, CO<sub>2</sub>, and H<sub>2</sub>O adsorption on clean polycrystalline graphite," *Carbon* 26, 507-514.

MARCHON, B., TYSOE, W.T., CARRAZZA, J., HEINEMANN, H. and SOMORJAI, G.A. (1988) "The reactive and kinetic properties of carbon monoxide and carbon dioxide on a graphite surface," *J. Phys. Chem.* 92, 5744.

HEINEMANN, H., SOMORJAI, G.A., PEREIRA, P. and CARRAZZA, J. (1989) "Catalytic gasification of graphite and chars," (presented at the 197th ACS National Meeting, Dallas, Texas, April 9-14, 1989) *American Chemical Society Division of Fuel Chemistry* 34 (1), 121.

HEINEMANN, H., PEREIRA, P., CSENCISITS, R. and SOMORJAI, G.A. (1990) "Steam gasification of graphite and chars at temperatures <1000 K over potassium-calcium-oxide catalysts," *J. Catal.* 123, 463. LBL-27655

HEINEMANN, H. and SOMORJAI, G.A. (1989) "Catalytic gasification fundamentals," in *Proceedings of the Ninth Annual Gasification and Gas Stream Cleanup Systems Contractors Review Meeting*, Vol. I.

HEINEMANN, H., PEREIRA, P. and SOMORJAI, G.A. (1992) "Catalytic steam gasification of coals," *Energy and Fuels* 6, 407. LBL-30609.

HEINEMANN, H., GINTER, D.M. and SOMORJAI, G.A. (1993) "Factors affecting the reactivity of chars and cokes during low temperature (640 °C) steam gasification," *Energy and Fuels* 7, 393. LBL-33064.



## **X. ACKNOWLEDGEMENTS**

The experimental work described in this report was carried out by the graduate students, post-doctoral fellows and visiting scientists listed here whose efforts are greatly appreciated: A.L. Cabrera, J. Carrazza, R. Casanova, D.J. Coates, R. Csencsits, F. Delannay, D.M. Ginter, B. Marchon, P. Pereira and W.T. Tysoe. Thanks are also due to the assistance and advice of Dr. R.T. Baker, Prof. J.W. Evans and Mr. J.J. Chludinsky. The work would not have been possible without the continued and encouraging support of the program managers at the Morgantown Energy Technology Center of the U.S. Department of Energy and particularly Dr. Sophia Lai, Dr. James Longanbach and Mr. Rodney Malone.